The importance of circulating iron-related proteins in mycobacterial infection – from mice to humans

Isabel Baptista de Oliveira
Master in Biochemistry
Department of Chemistry and Biochemistry
Faculty of Sciences and School of Medicine and Biomedical Sciences,
University of Porto
2024 / 2025

The importance of circulating iron-related proteins in mycobacterial infection – from mice to humans

Isabel Baptista de Oliveira

Dissertation carried out as part of the Master in Biochemistry
Department of Chemistry and Biochemistry
2024 / 2025

Supervisor
Maria Salomé Gomes, PhD
Leader of the Host Targets of Infection Group, i3S – Instituto de Investigação e Inovação em Saúde, Porto Portugal;
Full Professor at ICBAS – Instituto de Ciências Biomédicas Abel Salazar, University of Porto

Co-supervisor
Ana Carolina Moreira, PhD
Junior Researcher at i3S – Instituto de Investigação e Inovação em Saúde, Porto, Portugal;
Invited Assistant Professor at ICBAS – Instituto de Ciências Biomédicas Abel Salazar, University of Porto

Co-supervisor
Christopher Sundling, PhD
Principal Researcher and Team Leader at the Global Infections Research Group, Department of Medicine, Karolinska Institutet, Stockholm, Sweden
Associate Professor at Karolinska Institutet; Department of Medicine, Solna - Division of Infectious Diseases, Karolinska Institutet, Stockholm, Sweden

INSTITUTO DE INVESTIGAÇÃO E INOVAÇÃO EM SAÚDE
UNIVERSIDADE DO PORTO

KAROLINSKA INSTITUTET ANNO 1810
Karolinska Institutet

Funding

This project was conducted at i3S - Institute for Research and Innovation in Health, and Karolinska Institutet (Stockholm, Sweden).

This work was funded through National funds by Fundação para a Ciência e Tecnologia through the project "*IronCell2Cell: The macrophage-hepatocyte iron communication during mycobacterial infection*", identified with the following DOI: 2022.03635.PTDC.

Part of this project was carried out during an ERASMUS-funded student mobility at Karolinska Institutet (Stockholm, Sweden), between February and June 2025.

Acknowledgements

Começo por expressar a minha gratidão às instituições que marcaram o meu percurso académico. À FCUP e ao ICBAS, em especial ao seu corpo académico, agradeço a formação sólida e abrangente que me proporcionaram, cuja aprendizagem irá constituir para sempre o alicerce do meu conhecimento. Ao i3S, manifesto igualmente o meu reconhecimento pela forma como me acolheu durante a realização da dissertação de Mestrado e por me proporcionar um ambiente de investigação estimulante e enriquecedor.

Aos meus orientadores, deixo um profundo agradecimento. À Professora Salomé, pela oportunidade de integrar o seu grupo de investigação, pela orientação rigorosa e constante disponibilidade, e por ter criado um ambiente que me permitiu crescer enquanto formanda e pessoa.

À Carolina, agradeço de forma muito particular o apoio incondicional, o incentivo permanente e o desafio de participar no programa ERASMUS, uma experiência extremamente enriquecedora que dificilmente teria acontecido sem o seu encorajamento. Foi um privilégio partilhar estes anos contigo, ter-te como minha orientadora.

To my external supervisor Chris, I would like to thank you for welcoming me into your group and for giving me the opportunity to experience scientific research in an international context. Thanks to you, and to the entire *Inflammation and Immune Regulation during Infection* Team, I had an extraordinary ERASMUS experience. Thank you for your time, even with such a demanding schedule, and for showing me the importance of Bioinformatics in modern science. A special thank you to Hirofumi, Fariba, and Xubin for their patience and constant support.

Ao Óscar, agradeço a constante disponibilidade, a partilha de conhecimentos e os importantes conselhos. Tornas sempre os dias mais alegres, mesmo quando a vontade de sorrir não é muita.

À Leonor, agradeço todas as conversas e momentos que passamos juntas. Foste um apoio fundamental durante estes anos, não apenas como colega de investigação, mas também como amiga, cuja companhia e compreensão tornaram esta experiência mais significativa. À Mariana, agradeço também a amizade e o apoio permanente.

Aos restantes membros do grupo HoTI, Tânia, Gabriel e Clara, agradeço o apoio, a disponibilidade e os conselhos que contribuíram de forma significativa para o sucesso desta etapa.

À minha família, os agradecimentos nunca serão suficientes. Apenas direi que vos sou profundamente grata por tudo o que fizeram e continuam a fazer por mim, por estarem sempre ao meu lado. Em particular, agradeço aos meus pais e irmão, cujo esforço e dedicação tornaram possível a minha estadia na Suécia, um fator determinante para a concretização desta experiência académica.

Resumo

A tuberculose, causada por *Mycobacterium tuberculosis*, permanece uma das principais causas de mortalidade atribuídas a um único agente infecioso. Num contexto clínico, tanto o diagnóstico como a avaliação do risco de progressão da doença continuam a representar desafios de grande relevância. À semelhança do que ocorre com outros patogénios, as micobactérias perturbam significativamente a homeostase do ferro no hospedeiro. Face a estas alterações, devidamente documentadas, as proteínas associadas ao metabolismo do ferro têm vindo a ser estudadas como potenciais biomarcadores para a tuberculose. No entanto, dado que algumas dessas alterações não são exclusivas desta patologia, torna-se essencial identificar variações específicas em proteínas relacionadas com o metabolismo do ferro no decorrer da infeção.

Neste estudo, avaliou-se o impacto da infeção por *M. tuberculosis* e da sobrecarga de ferro nas proteínas do metabolismo do ferro em circulação, usando um modelo animal. Esta análise foi realizada com o objetivo de identificar assinaturas proteómicas exclusivas à infeção por *M. tuberculosis*. Os resultados mostraram que, no caso da ferritina, a principal proteína de armazenamento de ferro, os dois tipos de subunidades apresentaram uma regulação distinta perante estes estímulos: a ferritina-H revelou maior sensibilidade à infeção, enquanto a ferritina-L variou mais em função dos níveis de ferro.

Adicionalmente, foi realizada uma análise bioinformática exploratória abrangente, numa coorte de tuberculose, de forma a avaliar o potencial das proteínas plasmáticas associadas ao metabolismo do ferro como elementos diagnósticos e/ou preditivos da progressão da doença. Considerou-se um conjunto alargado de proteínas envolvidas no metabolismo do ferro, comparando indivíduos saudáveis com pacientes infetados e doentes com tuberculose ativa. Os resultados indicaram que as formas mais avançadas da doença se caracterizaram por uma acentuada regulação positiva de diversas proteínas, sobretudo mediadores inflamatórios, assim como de fatores relacionados com a imunidade e metabolismo do ferro, incluindo o recetor da transferrina, a ferritina-L e a interleucina-1β. Os perfis de distribuição das proteínas analisadas evidenciaram uma intensificação das vias de sinalização inflamatória e de retenção de ferro à medida que a severidade da doença aumenta.

No seu conjunto, estes resultados sugerem que proteínas associadas ao metabolismo do ferro, nomeadamente o recetor de transferrina e a ferritina, poderão constituir biomarcadores relevantes para a avaliação da progressão da tuberculose.

Futuramente, deverá ser explorado o papel mecanístico destas proteínas na patogénese da tuberculose.

Palavras-chave: Tuberculose, metabolismo do ferro, interação hospedeiro-patogénio, biomarcador, bioinformática

Abstract

Tuberculosis (TB), caused by *Mycobacterium tuberculosis*, is a leading cause of death from an infectious disease. In the context of TB management, the diagnosis and the assessment of risk of disease progression, are still major challenges. As with many other pathogens, infections by mycobacteria alters host iron homeostasis. Given these documented alterations, iron-related proteins are seen as potential biomarkers for TB. However, some of these iron metabolism alterations are not unique to TB, but common to other diseases, underlining the need to investigate specific alterations in iron metabolism-associated proteins in the context of this disease. In this study, the effect of both *M. tuberculosis* infection and iron overload on iron metabolism was assessed in animal experimental models. The results showed that in ferritin, a multimeric iron storage protein, the two types of subunits are differently regulated in response to these two stimuli: H-ferritin is more responsive to infection, while L-ferritin increase is more responsive to increased iron levels. A blind data-driven bioinformatics analysis was performed in a human TB cohort to study the potential of serum iron-related proteins as predictors of TB disease progression. With this analysis, a large set of iron metabolism-related proteins was studied, and healthy controls were compared to TB infection and disease patients. The results showed that severe TB disease exhibits a broad up-regulation of proteins, mainly inflammatory mediators, alongside immunity and iron-handling factors (transferrin receptor protein 1 (TFR1), L-Ferritin, Interleukin-1 β). In fact, the distribution profiles of the analysed proteins highlight amplification of inflammatory signalling and iron-sequestration pathways with increasing TB severity. Together, these results suggest that specific iron-related proteins, particularly TFR1 and ferritin, may serve as valuable indicators for assessing TB disease progression, possibly in combination with other markers. Future studies should focus on exploring their mechanistic role in TB pathogenesis.

Keywords: tuberculosis, iron metabolism, host-pathogen interaction, biomarker, bioinformatics

Table of Contents

List of Tables ix

List of Figures x

List of Abbreviations xi

Introduction 1

1. Mycobacterial Infection 2

1.1. Tuberculosis 2

1.2. Immune response to mycobacterial infection 4

2. Iron metabolism 5

2.1. Systemic Iron Homeostasis 5

2.2. Key Iron-binding proteins 7

3. Iron metabolism during mycobacterial infection 9

4. Iron-related proteins as potential biomarkers in TB management 11

Aim 14

Materials and Methods 16

Chemicals 17

Sera from experimental mouse models 17

Quantification of iron-related proteins by Enzyme-Linked Immunosorbent Assay (ELISA) 18

Samples from human cohort 19

Ferritin quantification in human plasma by ELISA 19

Analysis of plasma proteins by Proximity Extension Assay 20

Bioinformatic analysis of plasma protein expression 20

1. Exploratory data analysis 20

2. Differential Expression Protein Analysis 21

3. Software and packages 21

Statistical analysis 22

Results 23

1. Infection by *Mycobacterium tuberculosis* and iron overload induce distinct serum iron protein signatures in mice 24
1.1. Quantification of iron-related proteins in murine models of *M. tuberculosis* infection and iron overload 24
2. Iron metabolism proteins as predictors of TB disease progression in humans . 26
2.1. TB cohort characterization 27
2.2. Protein Filtering - Iron-related proteins 29
2.3. Exploratory data analysis 31
2.4. Evaluation of protein patterns according to TB severity 33
2.5. Differentially abundant proteins determination 35
2.6. Iron-related proteins abundance (with TBD subgroups) 37
Discussion 41
Conclusion 49
References 51

List of Tables

Table 1 - *Packages used during the bioinformatic analysis in R*.....22

Table 2 - *Demographic and clinical characteristics of the study participants* 27

Table 3 – *Relevant proteins under analysis.* 30

Table 4 - *12-protein signature associated with TB severity determined by Mousavian et al. (2022)* 33

List of Figures

Figure 1 - *Percentage change in TB incidence rate between 2015 and 2023, globally and by WHO region*. 2

Figure 2 - *Iron metabolism*. 6

Figure 3 - *Regulation of Ferritin Production*. 9

Figure 4 - *Biomarkers used in TB management.* 12

Figure 5 - *Schematic overview of the study aim.* 15

Figure 6 – *Quantification of iron-related proteins in the serum of mice infected with M. tuberculosis or iron overloaded.* 25

Figure 7 – *Heatmap of iron-related protein abundance across the tuberculosis (TB) cohort.* 31

Figure 8 - *Principal component analysis (PCA) of iron-related protein profiles across the tuberculosis cohort.* 32

Figure 9 - *Principal component analysis (PCA) of a 12-protein tuberculosis (TB) severity signature.* 33

Figure 10 - *Principal component analysis (PCA) of a 21-protein iron-related panel in the tuberculosis cohort.* 34

Figure 11 - *Systemic inflammatory markers by tuberculosis (TB) disease severity.* 35

Figure 12 – *Differential abundance analysis for TB diagnosis and disease progression.* 36

Figure 13 - *Distribution of iron-related and inflammatory proteins by tuberculosis (TB) status.* 38

Figure 14 – *Circulating ferritin levels before and after stratifying TB disease (TBD) by severity.* 39

List of Abbreviations

ALB	ALBUMIN
BACH1	TRANSCRIPTION REGULATOR PROTEIN BACH1
BMP6	BONE MORPHOGENETIC PROTEIN 6
BSA	BOVINE SERUM ALBUMIN
CCL2	C-C MOTIF CHEMOKINE 2
CFU	COLONY-FORMING UNIT
CRP	C-REACTION PROTEIN
CXCL10	C-X-C MOTIF CHEMOKINE 10
DMT1	DIVALENT METAL TRANSPORTER 1
EDTA	ETHYLENEDIAMINE TETRAACETIC ACID
ELISA	ENZYME-LINKED IMMUNOSORBENT ASSAY
ESR	ERYTHROCYTE SEDIMENTATION RATE
FeDx	IRON DEXTRAN
FPN	FERROPORTIN
FT	FERRITIN
FTH	H-FERRITIN
Fth1	H-FERRITIN GENE (MOUSE)
FTL	L-FERRITIN
HB	HEMOGLOBIN
HEPH	HEPHAESTIN
HIV	HUMAN IMMUNODEFICIENCY VIRUS
HJV	HEMOJUVELIN
HMOX1	HEME OXYGENASE 1
HRP	HORSERADISH PEROXIDASE
IFNG	INTERFERON-GAMMA
IFNGR	INTERFERON-GAMMA RECEPTOR
IGRA	INTERFERON-GAMMA RELEASE ASSAY
IL	INTERLEUKIN
IRE	IRON-RESPONSIVE ELEMENT
IRP	IRON REGULATORY PROTEIN
LAM	LIPOARABINOMANNAN
LTF	LACTOTRANSFERRIN
NNET	NEURAL NETWORK
NPX	NORMALIZED PROTEIN EXPRESSION

PAMP	PATHOGEN-ASSOCIATED MOLECULAR PATTERN
PBS	PHOSPHATE-BUFFERED SALINE
PCA	PRINCIPAL COMPONENT ANALYSIS
PCR	POLYMERASE CHAIN REACTION
PEA	PROXIMITY EXTENSION ASSAY
PRR	PATTERN-RECOGNITION RECEPTOR
SLC40A1	SOLUTE CARRIER FAMILY 40 MEMBER 1 (FERROPORTIN)
TB	TUBERCULOSIS
TBD	TUBERCULOSIS DISEASE
TBI	TUBERCULOSIS INFECTION
TMB	TETRAMETHYLBENZIDINE
TF	TRANSFERRIN
TFR	TRANSFERRIN RECEPTOR
TFR1	TRANSFERRIN RECEPTOR PROTEIN 1
TFR2	TRANSFERRIN RECEPTOR PROTEIN 2
Th1	T-HELPER 1 CELL
TNF	TUMOR NECROSIS FACTOR
TLR	TOLL-LIKE RECEPTOR
TST	TUBERCULIN SKIN TEST
UTR	UNTRANSLATED REGION

Introduction

1. Mycobacterial Infection

1.1. Tuberculosis

Tuberculosis is a chronic infectious disease caused primarily by *Mycobacterium tuberculosis* [1]. The disease typically affects the lungs (pulmonary TB) but can also affect other organs and tissues, including the lymph nodes, eyes and brain [2]. Despite being a preventable and usually curable disease, TB appears to have regained its status as the leading global cause of mortality from a single infectious agent, after being surpassed by COVID-19 in recent years [3]. According to the latest World Health Organization (WHO) data, an estimated 10.8 million people developed TB in 2023, with an estimated 1.25 million deaths attributable to the disease. In recent years, global TB incidence has shown declining trends, although progress has been uneven across regions (Figure 1) [3].

Figure 1 - *Percentage change in TB incidence rate between 2015 and 2023, globally and by WHO region*. Source: World health statistics 2025, WHO [3]

Regardless of this decreasing trend in disease incidence, it has been reported that about a quarter of the global population is estimated to be infected with *M. tuberculosis*, with the highest risk of developing TB disease being in the first 2 years after infection [3].

Infection rarely leads to disease. Only 5-10% of all people who become infected with *M. tuberculosis* develop clinical TB disease in their lifetime. The remaining 90-95% control the infection, leading to subclinical forms or ultimately, the clearance of the infection [1]. The risk of transitioning from infection to disease increases significantly when individuals suffer from other medical conditions, such as immunocompromise, diabetes or cancer [1].

Mycobacterium tuberculosis, the causative agent of TB, belongs to the genus *Mycobacterium*, a diverse group of bacteria that contains some of the most lethal human pathogens [4, 5]. Members of this genus are weakly Gram-positive, non-motile, catalase-positive, non-spore-forming bacilli with thick, lipid-rich, hydrophobic cell walls - a hallmark feature that contributes to their resilience and pathogenicity [4]. The genus includes obligate pathogens (such as *M. tuberculosis*), but also opportunistic pathogens, and environmental saprophytes [6, 7]. Unlike many bacterial pathogens that rely on secreted toxins to trigger acute inflammation and tissue destruction, *M. tuberculosis* presents a unique model of intracellular pathogenesis. It lacks classical virulence factors, yet is capable of long-term persistence in the host, often remaining latent for years without causing significant pathology or transmission [2]. Disease typically manifests only when host immune defenses become compromised and tissue destruction arises, mostly due to the host immune response [1]. TB is transmitted primarily via the airborne route. Infected individuals expel aerosolized droplets containing *M. tuberculosis* when coughing, sneezing, or even speaking [3]. These droplets can remain suspended in the air for prolonged periods and be inhaled by susceptible hosts. After inhalation, *M. tuberculosis* is phagocytosed by macrophages in the lung, where it can persist and replicate [8].

The diagnosis of TB is still a major bottleneck in the management of the disease, despite important improvements in recent years. Diagnostic methods include the direct detection of the causing bacteria, including correct species identification and drug susceptibility characterization, and indirect diagnosis, based on the host immune response to the pathogen [9].

The direct diagnosis of TB disease still relies heavily on conventional methods such as sputum smear microscopy for acid-fast bacilli and mycobacterial culture. While accurate, these approaches are labor-intensive and require long processing times. Over the last few years, they have increasingly been replaced by rapid molecular assays [9]. Among these is the GeneXpert MTB/RIF test, a nucleic acid amplification platform capable of detecting *M. tuberculosis* directly from sputum and simultaneously identifying

rifampicin resistance, a key first-line anti-TB drug. After diagnosis is established, repeated sputum smear microscopy and/or culture remain essential for monitoring the patient's microbiological response to therapy [1].

As previously mentioned, only a small percentage of individuals infected with *M. tuberculosis* develop disease. To identify TB infection, two immunological approaches are currently used: the Mantoux Tuberculin skin test (TST) and interferon-gamma (IFN-γ) release assays (IGRAs) [10]. TST is an *in vivo* test performed through a subcutaneous injection of an antigen (tuberculin or purified protein derivative) in the subject, who must then return to the clinical center for the determination of induration of the skin at the site of injection. IGRAs are blood tests that measure levels of IFN-γ following *in vitro* stimulation of human lymphocytes with two *M. tuberculosis* virulence factors [10]. While both assays evaluate the presence of a cell-mediated immune response, indicative of the presence of *M. tuberculosis* infection, neither can discriminate between infection and disease, nor predict the risk of progression from infection to disease [1]. This remains a major caveat in TB management, as it hampers the establishment of solid guidelines regarding therapeutic intervention.

1.2. Immune response to mycobacterial infection

Pattern-recognition receptors (PRRs) present in cells of the innate immune system, such as dendritic cells and macrophages, among others, recognize pathogen-associated molecular patterns (PAMPs), which are pathogen-specific motifs [11]. PRRs include Toll-like receptors (TLRs), which play an important role in recognizing intracellular and extracellular PAMPs [12]. The initial interaction between microbial PAMPs and PRRs can facilitate phagocytosis of the pathogen, followed by the maturation of the formed phagosome which, eventually, merges with lysosomes, forming phagolysosomes, responsible for bacterial degradation. Bacterial degradation involves the activation of hydrolytic enzymes and the formation of toxic nitrogen and oxygen radicals, contributing to pathogen clearance [13]. Additionally, PRR activation in innate immune cells leads to intracellular iron redistribution and the production of cytokines, which is essential for initiation of the inflammatory process [13]. These mechanisms constitute innate immunity, the first line of defense against pathogens. However, pathogenic mycobacteria are able to persist and replicate within macrophages by inhibiting their activation or/and resisting their mycobactericidal mechanisms [14]. An efficient immune response against this type of microorganism requires a tightly controlled mechanism that can contribute to

eliminate bacterial replication and at the same time limit potential tissue damage due to the inflammation process [15].

Cytokines produced when the host's innate immune system senses pathogens play a crucial role in connecting innate and adaptive immunity [12]. Interleukin (IL)-12 and Interferon γ (IFN-γ) are essential for regulating T-cell responses during mycobacterial infections. IL-12 acts as a bridge between these two phases of the immune response. During mycobacterial endocytosis, innate immune cells release IL-12, which activates $CD4^+$ T cells and promotes their differentiation into T-helper 1 (Th1) cells. IL-12 also activates $CD8^+$ T cells. Both Th1 and $CD8^+$ T cells produce large amounts of IFN-γ, a key cytokine for defending against mycobacteria, by activating antimicrobial mechanisms in macrophages. Additionally, Th1 cells secrete Tumor Necrosis Factor α (TNF-α), which ensures inflammation and synergizes with IFN-γ in increasing microbicidal activity. The coordinated action of IL-12 and IFN-γ is essential for controlling mycobacterial infections [12].

2. Iron metabolism

2.1. Systemic Iron Homeostasis

Iron is an essential element for numerous physiological processes. Iron is needed for erythropoiesis, hemoproteins (for biological functions such as oxygen binding and transport), for proteins responsible for oxidation-reduction reactions, DNA synthesis, gene regulation, among others [16, 17].

In humans, most body iron (~50%) is inside erythrocytes. Macrophages daily phagocyte old or senescent blood cells to efficiently recycle 20-25 mg of iron [18]. In fact, dietary iron absorption only accounts for 1-2 mg a day, which mostly compensates for iron losses from bleeding or skin desquamation [17]. Non-heme iron obtained from the diet is absorbed from the duodenal lumen by divalent metal transporter 1 (DMT1), a transporter located in the apical surface of enterocytes. Iron transported through DMT1 is in its ferrous form (Fe^{2+}), after ferric iron (Fe^{3+}) reduction in the duodenum's lumen, by duodenum cytochrome B. Internalized Fe^{2+} can then be exported from enterocytes to the bloodstream via efflux protein ferroportin (FPN) [19]. The export of iron happens along with its re-oxidation to Fe^{3+} by hephaestin, allowing its binding to the serum iron transporter protein transferrin.

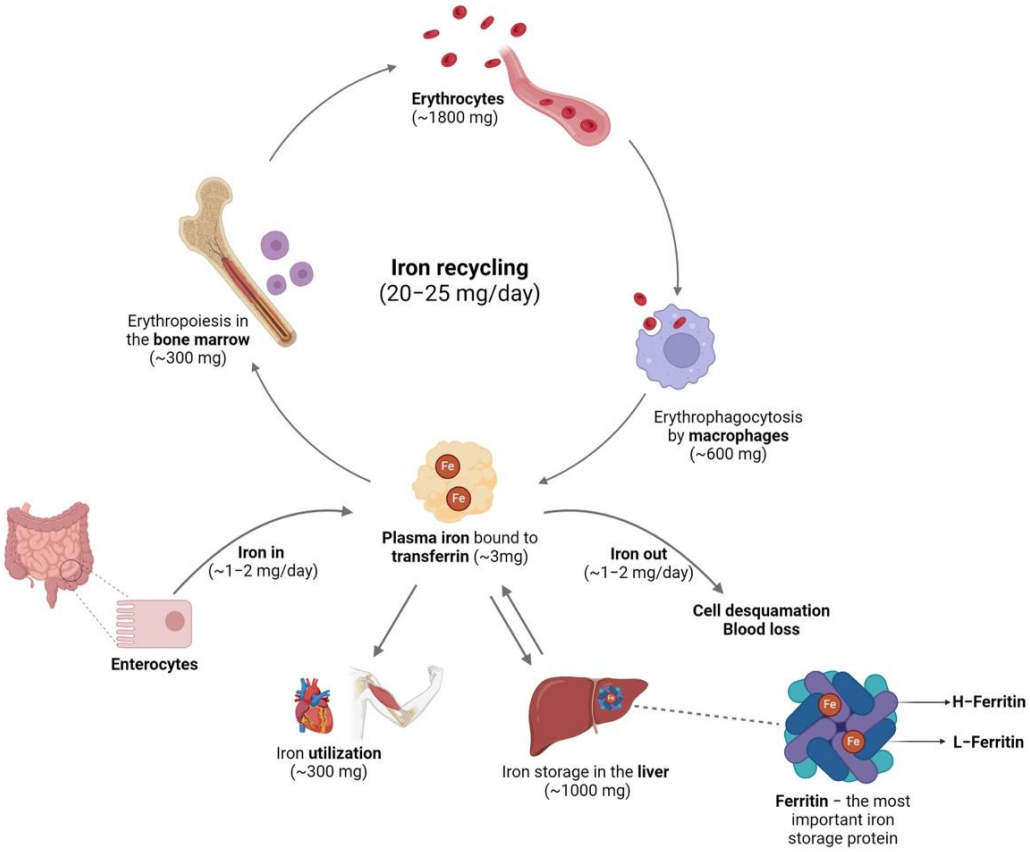

Figure 2 - *Iron metabolism*. To ensure iron homeostasis, mammals tightly regulate iron storage, absorption, transport, and recycling. Iron losses due to cell desquamation and blood loss are promptly compensated by iron dietary absorption. The remaining iron requirements are secured by iron recycling. Circulating iron, bound to transferrin, is required for erythropoiesis and recycled from senescent or old red blood cells by macrophages. Regarding storage, iron is kept in hepatocytes, within ferritin. Figure obtained from Fonseca et al., 2023 [20]

While it is true that all living forms depend on iron, it is no less true that this element is also potentially toxic. Therefore, it is essential to tightly regulate iron levels both systemically and at the cellular level. Hepcidin, a protein produced by the liver, serves as the master regulator of systemic iron homeostasis [21]. It controls serum iron levels by promoting the degradation of FPN in iron-absorbing enterocytes and iron-recycling macrophages [19]. In the case of iron excess, hepcidin is stimulated, preventing iron export to circulation by negatively regulating FPN [18]. In the next section, two key players in iron metabolism and regulation will be characterized: transferrin and ferritin. Transferrin (TF) is the major responsible for iron transport, binding bioavailable iron in circulation, delivering it to several tissues and preventing it from generating oxidative stress [22]. On the other hand, ferritin (FT) is the main intracellular iron storage protein. It sequesters excess iron in a soluble and non-toxic form, releasing it when needed for metabolic processes [19]. Together, TF and FT contribute to iron homeostasis, ensuring

that enough iron is available for vital functions, while preventing iron overload and associated cellular damage.

2.2. Key Iron-binding proteins

2.2.1. Transferrin

After reaching the bloodstream, iron is transported throughout the body tightly bound to transferrin (TF) [23]. TF is a 75-80 kDa protein with two binding sites for ferric iron [22]. It is mainly produced in the liver and has an 8-day half-life in the serum [24]. TF has two functions: 1) to deliver bioavailable iron to different tissues and 2) to prevent the formation of toxic radicals [22].

Human serum TF has a typical concentration of 200–300 mg/dL, which decreases during hepatic dysfunction or inflammation. TF's remarkable affinity for iron allows it to bind free iron in the bloodstream, preventing toxicity, assuring that most serum iron is bound to TF. Serum TF exists in three forms: non-iron-bound (apo-TF), monoferric, or diferric (holo-TF) [24]. In a healthy human, only one-third of TF is typically iron-saturated [22].

TF binds to transferrin receptors TFR1 and TFR2 to deliver iron to cells. The transferrin receptor (TFR) is a homodimeric membrane protein that mediates iron uptake into the cell. Each subunit possesses one binding site for the iron carrier protein TF. While TFR1 is almost ubiquitously expressed across the organism, TFR2 is restricted to the liver, duodenum, and erythroid cells and it has less affinity to TF than TFR1 [22, 25]. After binding, the TF-TFR complex is internalized via receptor-mediated endocytosis. Acidification of the endosome releases iron, and TF is recycled to the extracellular space. A soluble form of the transferrin receptor, obtained by proteolytic cleavage of the membrane-bound receptor, circulates in plasma and can be quantitatively measured. This soluble form reflects the degree of cellular TFR expression [26].

2.2.2. Ferritin

If not exported by FPN or incorporated in iron-dependent enzymes, intracellular iron is stored in ferritin (FT), the key intracellular provider of bioavailable iron [19]. Recognized as the essential protein for cellular iron storage, mammalian FT is a large, spherical molecule formed by 24 units comprising two types of peptides: heavy (FTH) and light (FTL) chains with approximately 20 kDa each [27]. This cytosolic protein, which can store

up to 4500 atoms of Fe^{3+}, can have different FTH/FTL ratios in different tissues and organs, generally adding up to 450 kDa in apoferritin, the iron-free protein [28, 29]. FTH has an active role in detoxification by the conversion of Fe^{2+} to Fe^{3+}, through a ferroxidase site, which is a step required for iron incorporation inside the FT cage. FTL does not have this ferroxidase domain but plays an important role in conferring stability to FT and assists in iron incorporation by increasing the iron turnover in the catalytic center. Therefore, tissues requiring higher anti-oxidative capacity have increased levels of FTH, while FTL is predominantly found in tissues focused on iron storage [27].

FT can also be found in the serum. Regarding its FTH/FTL content, serum FT is described in some studies as having a high FTL content, in contrast to the fewer number of FTH subunits, resulting in a small concentration of iron [30, 31]. Furthermore, two key hypotheses have been proposed regarding FT cellular export: one suggests that FT is passively released as a result of the death of damaged cells [32], while another proposes that macrophages, and other cells, actively secrete FT via non-classical secretory autophagy and multivesicular body-exosome pathways [30].

As a key player in iron metabolism, FT's levels must be tightly controlled. The regulation of FT expression happens mainly at a post-transcriptional level and is highly dependent on cellular iron levels. FT production is controlled by iron regulatory proteins (IRP) 1 and 2. When cellular iron levels are low, IRPs bind to the iron-responsive element (IRE) in the untranslated regions of H- and L-ferritin mRNA, blocking translation at the initiation stage. In fact, IRP1 switches between two conformations based on iron availability: in iron-rich environments, it adopts a cytosolic aconitase form, while in iron-scarce environments it shifts to a configuration that can bind to the IRE, as reviewed in Moreira, Mesquita [33]. IRP2 is degraded in high-iron conditions [27]. This regulation is further explained in Figure 3. In addition to iron, FT levels are controlled by protein degradation through a process called ferritinophagy [34].

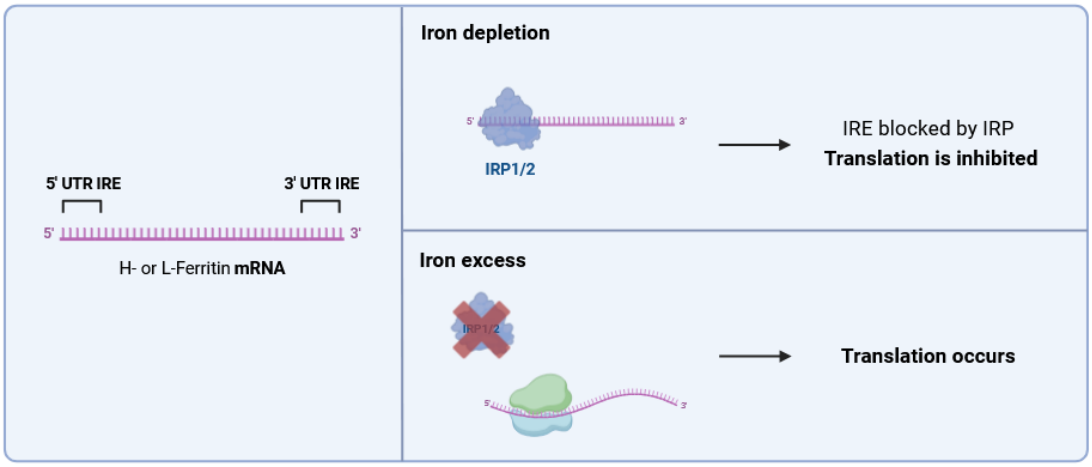

Figure 3 - *Regulation of Ferritin Production*. FT production is highly dependent on iron levels. IRE is located in the 5' untranslated region (UTR) of H- or L-ferritin mRNA. In iron depletion, iron regulatory proteins (IRPs) bind to the iron-responsive element (IRE), blocking mRNA translation. When iron levels are high, IRPs are inactivated: IRP1 undergoes a conformational change, while IRP2 is degraded. This prevents IRPs from binding to IREs, enabling mRNA translation to proceed. Figure created with Biorender.com.

By storing iron, FT plays a vital role as one of the most important agents in intracellular iron detoxification: through the incorporation of iron, this protein prevents reactive oxygen species formation. FT is also involved in immunomodulation [27], as will be explored in the next section of this report.

3. Iron metabolism during mycobacterial infection

As previously mentioned, iron is needed in all species. For that reason, iron acquisition is a key element in pathogens' survival and proliferation in the host. After all, the pathogenicity of a microorganism is directly related to its ability to adjust and survive within the host [35, 36]. To utilize the pathogen's need for iron for its defense, the host has developed a series of mechanisms that sequester iron from the site of infection. The removal of vital nutrients from pathogens, such as iron, is seen as an effective host defense strategy - hence, the concept of nutritional immunity [37, 38].

However, to ensure their survival despite this iron scarcity, pathogens have developed a series of mechanisms to obtain iron within the host [39]. Microbes secrete iron chelator molecules - siderophores - that can bind ferric iron with high affinity [40, 41]. These molecules can obtain iron from host iron-binding proteins, heme-binding proteins and iron transporters [41]. Yet, siderophores are non-specific to the microorganism that releases them, meaning that neighboring microbes can acquire these molecules. Additionally, siderophores can be eliminated by the host through specific binders, like

lipocalin-2 [42]. Siderophores were not found in *M. tuberculosis*-infected tissues, as reported by Lambrecht and Collins [43], suggesting the existence of alternative acquisition mechanisms for this pathogen, *in vivo*. A study by Tullius, Harth [44] provides further evidence that siderophores may not be essential for *M. tuberculosis* infection outcome, demonstrating that a strain unable to synthesize siderophores maintained its ability to invade and multiply within macrophages. This suggests a different pathway to iron acquisition. The dependence of *M. tuberculosis* on iron for growth has been clearly established. It has been shown, both in humans and in animal models, that host iron overload correlates positively to an efficient infection and progress of the mycobacterial disease [45-47]. The converse is also true, with iron chelation or starvation correlating with less bacterial growth [48]. Thus, it is not surprising that host defense mechanisms include removing iron from circulation to limit its accessibility to invading pathogens.

It is well-established that infection and inflammation have a significant impact on iron homeostasis. Pathology may be exacerbated by iron imbalance, particularly in cases of chronic or persistent infections. Our group has previously shown the impact that different pathogens have on iron homeostasis [49-51]. During *M. tuberculosis* infection, differences in serum levels of proteins involved in iron metabolism, including TF and FT, have been reported [52]. These changes reflect the host's attempt to regulate iron availability as part of the immune response to infection.

Beyond its regulation by systemic iron status, hepcidin is also strongly induced by inflammation, with IL-6-dependent signaling constituting a major pathway activated during bacterial infection. Consequently, hepcidin induces the degradation of FPN, leading to the retention of iron within macrophages and a decrease in intestinal iron absorption. This process drastically lowers serum iron levels, a condition referred to as hypoferremia [53]. In *Mycobacterium avium* infection this regulatory protein does not appear to play a significant role in the interaction between host and pathogen. Previous studies show that mice infected with this pathogen do not exhibit notable changes in hepatic hepcidin expression [54, 55]. In contrast, mice infected with *M. tuberculosis* exhibit suppressed hepcidin expression at later stages of infection. Furthermore, the absence of hepcidin does not affect susceptibility to *M. tuberculosis* [56].

Our group has previously reported that FT has a central role in this iron redistribution [49]. Previous studies, including work from our group and later supported by others, demonstrated that primary mouse macrophages infected *in vitro* with *M. avium* show increased expression of FTH, while FTL levels remain unchanged [57]. These findings suggest a potential involvement of FTH in modeling the outcome of mycobacterial

infections *in vivo*. Supporting this, a mouse model with a myeloid cell-specific deletion of the *Fth1* gene was used and found that FTH contributes to protection during *M. tuberculosis* infection, as evidenced by increased organ burden, extrapulmonary dissemination and decreased survival [58]. This highlights its role in the host's defense mechanisms. Our group has also previously demonstrated the crucial role of myeloid-derived FTH in iron redistribution during a mycobacterial infection [49]. FTH transcription is responsive to inflammatory stimuli, including TNF-α and IL-6 [36, 59]. Consequently, one of the iron-related hallmarks of the inflammatory response is hyperferritinemia (rise in the serum levels of FT). In fact, FT is seen as an acute phase protein, an inflammation and infection marker [36].

4. Iron-related proteins as potential biomarkers in TB management

As mentioned previously, only a small proportion of individuals infected with *M. tuberculosis* will develop disease. Thus, both the detection of those infected and the identification of those that will develop disease, are major challenges, in the context of TB management. The process of identifying individuals infected with *M. tuberculosis* can take several weeks and, as already discussed, relies on a combination of clinical symptoms, radiological findings, and the detection of *M. tuberculosis* components or live bacteria [51, 59]. On the other hand, immunological assays, which screen for Mtb-specific T-cell memory, fail to predict progression to TB disease.

Given this inefficiency, new solutions are needed, to improve both the diagnosis and prognosis of these patients [60]. Circulating biomarkers would represent a good solution to this problem and are sought by many researchers.

According to the Food and Drug Administration (USA) [61], a biomarker is "*a defined characteristic that is measured as an indicator of normal biological processes, pathogenic processes or responses to an exposure or intervention*". According to Califf [62], biomarkers can be broadly classified depending on their clinical application: (i) susceptibility/risk biomarkers, to indicate the potential for developing a disease in an individual not currently affected; (ii) diagnostic biomarkers, which help detect or confirm the presence of a disease or condition; (iii) monitoring biomarkers, measured repeatedly to assess the status of a disease or the effects of treatment; (iv) prognostic biomarkers, that provide information about the likely course of a disease, including recurrence or

progression; (v) predictive biomarkers, to identify individuals more likely to respond to a particular therapy; (vi) pharmacodynamic/response biomarkers, that show that a biological response has occurred after a medical intervention; and (vii) safety biomarkers, which indicate the likelihood or presence of toxicity associated with a treatment [62]. The exploration of biomarkers for TB is not necessarily new – both host and pathogen biomarkers have been studied. The latter includes the detection of both antigen and DNA; while the host-based comprise a wide range of biomarkers such as cytokines and chemokines, RNA, other proteins, and signatures that combine multiple markers [60]. In the TB context, biomarkers can be used as a diagnostic tool, as prognostic tests for the risk of progression to disease, and to evaluate treatment response (Figure 4).

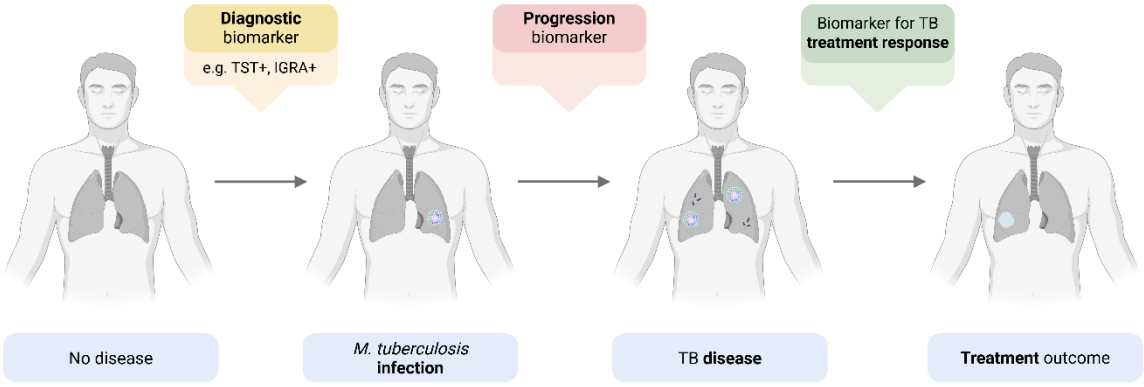

Figure 4 - *Biomarkers used in TB management.* Schematic representation of the tuberculosis (TB) disease spectrum, highlighting the stages appropriate for biomarkers for diagnosis (e.g., TST, IGRA), disease progression, and treatment response. Figure created in Biorender.com.

Most TB biomarkers studied are host-derived, including proteomic, transcriptomic, or metabolomic markers, as well as combinations of these in multi-omic approaches [63]. Proteomics is regarded as the analysis of "*protein composition, structure, expression, modification status, and the interactions and connections between proteins at an overall level*" [64]. This type of analysis complements genomics and transcriptomics, as they disregard post-transcriptional changes. Proteomics is a key element in the study of the complex, interconnected pathways, networks, and molecular systems – hence its importance in the discovery and development of biomarkers [64].

Regarding TB, several host-based diagnostic biomarkers associated with a dysregulated and exacerbated immune system response have been identified [60]. Regarding cytokine response, the measurement of IFN-γ levels after stimulation with *M. tuberculosis*-specific antigens (IGRA), established itself as an important step in the diagnosis of current or prior *M. tuberculosis* infection, despite the inaccuracy for TB

disease. Antigen-specific antibodies against *M. tuberculosis* are the most studied biomarker category for pulmonary and extrapulmonary TB. However, once again, they have not revealed themselves as useful for distinguishing between TB infection and disease [60]. According to the latest WHO guidelines for TB diagnosis [65], the detection of antigens for lipoarabinomannan (LAM), a *M. tuberculosis* cell wall glycolipid, in urine is also currently used in HIV-positive patients. LAM-antigen detection is not suitable as general diagnostic tests for TB, due to its suboptimal sensitivity [65, 66]. Nonetheless, as previously described, iron homeostasis is disrupted during *M. tuberculosis* infection and disease, meaning that biomarkers related to iron redistribution, including FT and TF, present themselves as possibly useful tools in the evaluation of TB disease progression. In fact, a previous study evaluated the concentration of iron-related biomarkers in a large cohort of patients and used them in a prediction model to diagnose TB disease [52]. In this study, Dai and colleagues evaluated the three main iron biomarkers (serum iron, FT and TF) and combined them in a neural network (NNET) model, which was able to discriminate TB disease with 70% sensitivity and 92% specificity in a testing cohort. Seen as a powerful computational tool for identifying patterns and making predictions based on complex datasets, the NNET model uses machine learning mechanisms to improve diagnosis accuracy and reliability. However, this model had a modest sensitivity and the study only referred to two cohorts, which may not fully represent TB patients globally [52]. Thus, there is a lot of room for improvement regarding iron-related biomarkers. Inflammation-induced disturbances in host iron homeostasis occur following infections by various pathogens, which can reduce the specificity of iron metabolism players as diagnostic biomarkers for TB [41]. To address this limitation, recent studies have explored combining multiple iron metabolism indicators to enhance specificity [52]. Another promising strategy is pairing these biomarkers with *M. tuberculosis*-specific biomarkers for improved diagnostic accuracy [41].

Aim

Iron-related proteins are potential biomarkers for TB infection and disease. However, alterations in iron metabolism are not unique to TB. Elevated ferritin levels, for example, also occur in other conditions such as iron overload. A deeper investigation of iron metabolism-associated proteins in the context of TB is needed. This will allow the identification of biomarkers to guide diagnosis, prognosis and treatment success, while improving our understanding of their roles in pathogenesis.

Building on this rationale, the present study aimed to:

(1) compare the impact of *M. tuberculosis* infection and iron overload on the circulating levels of specific iron-related proteins, in mice;

(2) evaluate the potential of serum iron-related proteins as predictors of TB disease progression in humans.

To address Aim 1, circulating iron-related proteins were quantified in serum samples from C57BL/6 mice infected with different *M. tuberculosis* strains, as well as from mice subjected to experimental iron overload. For Aim 2, we performed a bioinformatic analysis of plasma proteomics data from a TB cohort comprising healthy controls, individuals with *M. tuberculosis* infection, and patients with TB disease. The proteomic panel was restricted to a subset of proteins selected based on their involvement in iron metabolism and/or their relevance to TB disease outcome and host immune-related response.

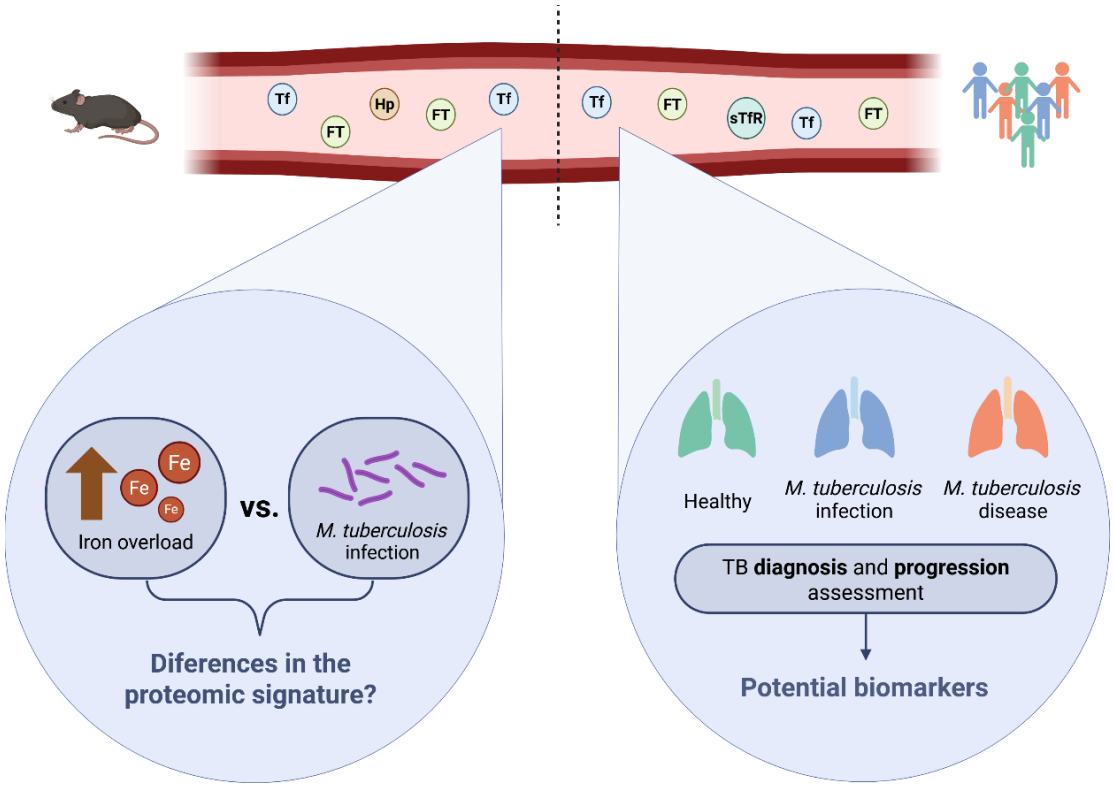

Figure 5 - *Schematic overview of the study aim.* Comparison of the effects of iron overload and Mycobacterium tuberculosis infection on iron-related proteins in a mouse model (left) and evaluation of plasma iron-associated proteins as potential biomarkers for TB diagnosis and disease progression in a human cohort (right). Figure created in Biorender.com.

Materials and Methods

Chemicals

Unless stated otherwise, chemicals and reagents were acquired from Sigma-Aldrich (St. Louis, MO, USA).

Sera from experimental mouse models

C57BL/6 mice were bred and housed under specific pathogen-free conditions at the Instituto de Investigação e Inovação em Saúde (i3S) animal facility. The mice were kept inside ventilated cages with HEPA filters and fed with sterilized food and water ad libitum. All procedures were carried out by people certified by FELASA (Federation for Laboratory Animal Science Associations) under the approval of DGAV (Direção-Geral de Alimentação e Veterinária).

Infection with *M. tuberculosis* was performed by Rute Gonçalves from the Immune Regulation Group at i3S. Mice were infected, by the aerosol route, with clinical *M. tuberculosis* isolates derived from TB patients with mild (4I2) or severe (6C4) disease, or with a hypervirulent reference strain (HN878). Infection level was defined based on the bacterial burden at 3-days post-infection (p.i.): below 200 CFUs was categorized as low dose, corresponding to HN878 infection, and exceeding 500 CFUs was determined as high dose, corresponding to the other strains. Mice infected with the 4I2 isolate were euthanized at 90 days p.i., whereas those infected with 6C4 or HN878 were sacrificed at 30 days p.i. Blood was collected via cardiac puncture. In addition, blood samples were collected from control, non-infected, mice.

Dr. Tiago Duarte, from the Hematopoiesis and Microenvironments Group at i3S, kindly provided serum samples collected from C57BL/6 mice (~12 weeks old) that received one dose of either Iron Dextran (FeDx) (0.5 g Fe/kg body weight) or Dextran (control). At 24h post injection, after a 5-hour starvation period, blood was obtained via retro-orbital bleeding under anesthesia with isofluorane. Animals were then euthanized by cervical dislocation.

After collection, the blood was allowed to clot at room temperature and centrifuged at maximum speed for 10 minutes to isolate the supernatant, the serum. All serum samples were stored at -80 °C until further use.

Quantification of iron-related proteins by Enzyme-Linked Immunosorbent Assay (ELISA)

Mouse serum concentrations of ferritin, transferrin, and haptoglobin were measured using three different commercial ELISA kits, each specific to the target protein. Ferritin levels were assessed using the Mouse Ferritin ELISA Kit (catalog No. ab157713, Abcam, Cambridge, United Kingdom), transferrin using the Mouse Transferrin ELISA Kit (Colorimetric) (catalog No. NBP2-60636, Novus Biologicals, Littleton, CO, USA), and haptoglobin using the Mouse Haptoglobin ELISA Kit (catalog No. ab157714, Abcam, Cambridge, United Kingdom). All assays were performed according to the manufacturers' instructions. Samples were appropriately diluted and analysed in duplicate, and absorbance was measured using a SynergyTM Mx Multi-Mode Microplate Reader with Gen5 software (BioTek, Winooski, VT, United States).

Serum concentrations of H- and L-ferritin in mice were quantified with a homemade sandwich ELISA, based on antibodies kindly provided by Paolo Santambrogio and Sonia Levi, Università Vita-Salute San Raffaele, Milano, as described previously [67]. Briefly, 96-well plates were coated overnight at 4 °C with 100 µL/ well of a capture antibody (anti-mouse H- or L-ferritin) diluted in carbonate buffer (pH 9.6). The plates were then washed and blocked with 100 µL/well of blocking buffer (2% BSA in PBS) for 1h at room temperature. After washing, 100 µL of diluted serum samples or standards (recombinant mouse H- or L-ferritin) were added to each well and incubated for 2 hours at room temperature. Plates were washed again and incubated with 100 µL/well of a biotinylated detection antibody (anti-mouse H- and L-ferritin) for 1h. Following another wash step, 100 µL of Streptavidin-HRP conjugate was added and incubated for 1h. The reaction was done with TMB substrate, stopped with H_2SO_4 2N, and absorbance was measured at 450 nm and 570 nm (to evaluate background absorbance) using a SynergyTM Mx Multi-Mode Microplate Reader and Gen5 software (BioTek, Winooski, VT, USA). H- and L-ferritin concentrations were determined using a standard curve generated from known concentrations of the respective recombinant standards.

ELISA data were expressed as fold change relative to controls. For each experimental condition, the concentration measured in individual animals was normalized to the mean concentration of the control group, which was set to 1 in all graphical representations.

Samples from human cohort

The study was registered and granted ethical approval by the Swedish Ethical Review Board, EPN number 2019-05438. All study participants were adults and, after being provided with written and verbal information, signed informed consent forms.

Samples, clinical data, and demographic information were obtained from individuals recruited and enrolled at Karolinska University Hospital in Stockholm.

Adult patients (over 18 years old) were recruited from the TB department at Karolinska University Hospital (Stockholm) from 2021 to 2023. Patients were considered eligible if they met one of the following criteria: 1) had TB disease sampled within 1 week of anti-TB treatment initiation. TB disease was identified either through a positive microbiological verification via *M. tuberculosis* culture or, if the result was negative, the diagnosis relied on other positive microbiological tests (microscopy or PCR), along with consistent clinical and radiological findings and a positive response to TB treatment; 2) had TB infection with a positive IGRA result identified through contact investigations or migrant screening, in which TB disease had already been excluded. Healthy controls were selected from adult students and staff with no known prior exposure to TB, no significant co-morbidities, and no evidence of immunosuppression.

Data on symptoms and blood chemistry were extracted from electronic medical records, while additional details, such as prior health status and TB exposure, were collected through questionnaires administered during patient enrollment in the study. For all participants, data on prior exposure to individuals with TB disease were collected, as well as co-morbidities, current medication, and results from radiological, biochemical, and microbiological tests. In TB disease cases, clinical symptoms were documented, and patients were categorized as having either pulmonary or extrapulmonary TB.

Ferritin quantification in human plasma by ELISA

Ferritin levels were quantified in human plasma-EDTA obtained from patients with TB infection and disease using the Invitrogen Human Ferritin ELISA Kit (catalog No. EHFTL, Invitrogen, Massachusetts, USA). All steps of the protocol were carried out as described in the manufacturer's instructions, including the use of the appropriate dilutions. Absorbance was measured at 450 nm and 570 nm (to evaluate background absorbance) in a Multiskan SkyHigh Microplate Spectrophotometer (Thermo Fisher Scientific, Massachusetts, USA).

Analysis of plasma proteins by Proximity Extension Assay

Venous blood samples were collected into heparin or EDTA-coated vacutainer tubes and promptly delivered to the laboratory. After centrifugation at 670 g for 8 minutes, the plasma was separated, aliquoted and stored at -80 °C until analysis. More than 5400 proteins in the plasma were quantified using the Olink Proximity Extension Assay (PEA) (Olink Proteomics AB, Uppsala, Sweden). PEA is a high-throughput technique in which matched pairs of oligonucleotide-labeled antibodies bind to their target antigens in a pairwise manner. After the antibody binding, the matched oligonucleotides are brought into proximity and, with the use of a DNA polymerase, a PCR target sequence is created, amplified, detected and quantified [68]. The resulting data was then quality controlled and normalized using internal controls, transformed into Normalized Protein Expression (NPX) values and represented as a relative quantification unit on a $\log_2$ scale. The assay was conducted at the Translational Plasma Profile Facility, in SciLifeLab (Stockholm, Sweden).

Bioinformatic analysis of plasma protein expression

1. Exploratory data analysis

1.1. Data curation and preprocessing

NPX data generated with the Olink Proximity Extension Assay were curated by Protein Atlas staff, from the SciLifeLab, before being shared for analysis. According to what was documented, curation included the calculation of the limit of detection (LOD) using the *OlinkAnalyze* R package, the detection and exclusion of outlier samples, and the removal of non-essential metadata columns.

Quality control summaries were generated in R software. For each assay, the number and percentage of measurements above the LOD, and the mean and standard deviation of LOD values were computed. Feature selection, censoring, imputation, and data exports were also performed in R. Assays were retained if, in at least one clinical subgroup, the proportion of measurements above LOD was ≥ 50%. For values flagged as below LOD, NPX was replaced with the corresponding LOD value (censoring at LOD). Missing NPX values were then imputed within each subgroup using the median NPX for that subgroup and assay; if any values remained missing after this step, they were imputed with the overall assay median.

1.2. Heatmap of protein expression

A heatmap was generated using the preprocessed NPX values, to visualize the global expression pattern across samples and to assess potential clustering based on the experimental groups. Values were visualized using the *ComplexHeatmap* package with a blue-white-red diverging scale.

1.3. Principal Component Analysis (PCA)

Principal Component Analysis (PCA) was performed to reduce data dimensionality and identify sample clustering patterns or potential batch effects. The first two principal components were plotted and interpreted.

2. Differential Expression Protein Analysis

Differential expression analysis was performed to identify proteins significantly associated with the clinical groups. Differential expression analysis was performed using the *limma* package. NPX values were already $\log_2$-transformed, filtered to remove proteins with excessive missing values, and normalized across samples. A linear model was fitted to each protein to assess group differences, and empirical Bayes moderation was applied to shrink variance estimates across proteins. Moderated *t*-statistics were computed for predefined contrasts and *p*-values were adjusted. Proteins with an adjusted p-value < 0.05 and a fold-change above a specified threshold were considered differentially expressed.

3. Software and packages

All analyses were performed in R version 4.4.3 (R Foundation for Statistical Computing, Viena, Austria). The following R packages were used:

Table 1 - *Packages used during the bioinformatic analysis in R*

R package	Source
OlinkAnalyze	Olink-Proteomics. (2025). *OlinkAnalyze (v4.2.0)* [R package]. GitHub. https://github.com/olink-omics/
ggplot2	Wickham, H. (2016). *ggplot2: Elegant Graphics for Data Analysis*. Springer-Verlag. https://ggplot2.tidyverse.org
limma	Ritchie, M. E., Phipson, B., Wu, D., Hu, Y., Law, C. W., Shi, W., & Smyth, G. K. (2015). limma powers differential expression analyses for RNA-sequencing and microarray studies. *Nucleic Acids Research, 43*(7), e47. https://doi.org/10.1093/nar/gkv007
tidyverse	Wickham, H., Averick, M., Bryan, J., Chang, W., McGowan, L. D. A., François, R., ... Yutani, H. (2019). Welcome to the tidyverse. *Journal of Open Source Software, 4*(43), 1686. https://doi.org/10.21105/joss.01686
ComplexHeatmap	Gu, Z., Eils, R., & Schlesner, M. (2016). Complex heatmaps reveal patterns and correlations in multidimensional genomic data. *Bioinformatics, 32*(18), 2847–2849. https://doi.org/10.1093/bioinformatics/btw313
circlize	Gu, Z., Gu, L., Eils, R., Schlesner, M., & Brors, B. (2014). circlize implements and enhances circular visualization in R. *Bioinformatics, 30*(19), 2811–2812. https://doi.org/10.1093/bioinformatics/btu393
ggrepel	Slowikowski, K. (2024). *ggrepel: Automatically position non-overlapping text labels with 'ggplot2'* (R package version 0.9.5). https://CRAN.R-project.org/package=ggrepel
edgeR	Robinson, M. D., McCarthy, D. J., & Smyth, G. K. (2010). edgeR: A Bioconductor package for differential expression analysis of digital gene expression data. *Bioinformatics, 26*(1), 139–140. https://doi.org/10.1093/bioinformatics/btp616
dyplr	Wickham, H., François, R., Henry, L., & Müller, K. (2023). *dplyr: A grammar of data manipulation* (R package version 1.1.4). https://CRAN.R-project.org/package=dplyr
tidyr	Wickham, H., & Girlich, M. (2024). *tidyr: Tidy messy data* (R package version 1.3.1). https://CRAN.R-project.org/package=tidyr

Statistical analysis

Data statistical analysis is expressed as means ± standard deviation. Statistical analyses were performed using GraphPad Prism 8.0.1 (GraphPad Software, La Jolla, CA, USA) for mice serum samples, and R version 4.4.3 (R Foundation for Statistical Computing, Vienna, Austria) for human plasma data. Unless stated otherwise, multiple comparisons between experimental groups were performed using an ordinary one-way ANOVA, and the p-value was determined. Comparisons were considered statistically significant when $p < 0.05$.

Results

1. Infection by *Mycobacterium tuberculosis* and iron overload induce distinct serum iron protein signatures in mice

Infection has a clear influence on the host's iron metabolism [5, 49, 69]. Among other findings, our group has previously reported that, during a mycobacterial infection, FTH produced in myeloid cells was released into the bloodstream and modulated iron redistribution in the liver [49]. Similarly, Dai *et al.* [52] found that circulating FT levels were elevated in humans with TB, with higher concentrations associated with greater disease severity [52]. However, increased circulating FT levels are also observed in iron overload diseases [70, 71]. In this part of the work, we aimed at identifying differences in the impact of infection versus iron overload, on circulating iron metabolism-related proteins. The long-term goal would be to define a specific set of iron-related proteins or their specific characteristics, that could distinguish mycobacterial infection from other diseases, in a clinical setting.

1.1. Quantification of iron-related proteins in murine models of *M. tuberculosis* infection and iron overload

Ferritin (and its L- and H-subunits), transferrin, and haptoglobin, were quantified in sera from C57BL/6 mice previously rendered iron overloaded or infected with *M. tuberculosis* of different virulences (Figure 6).

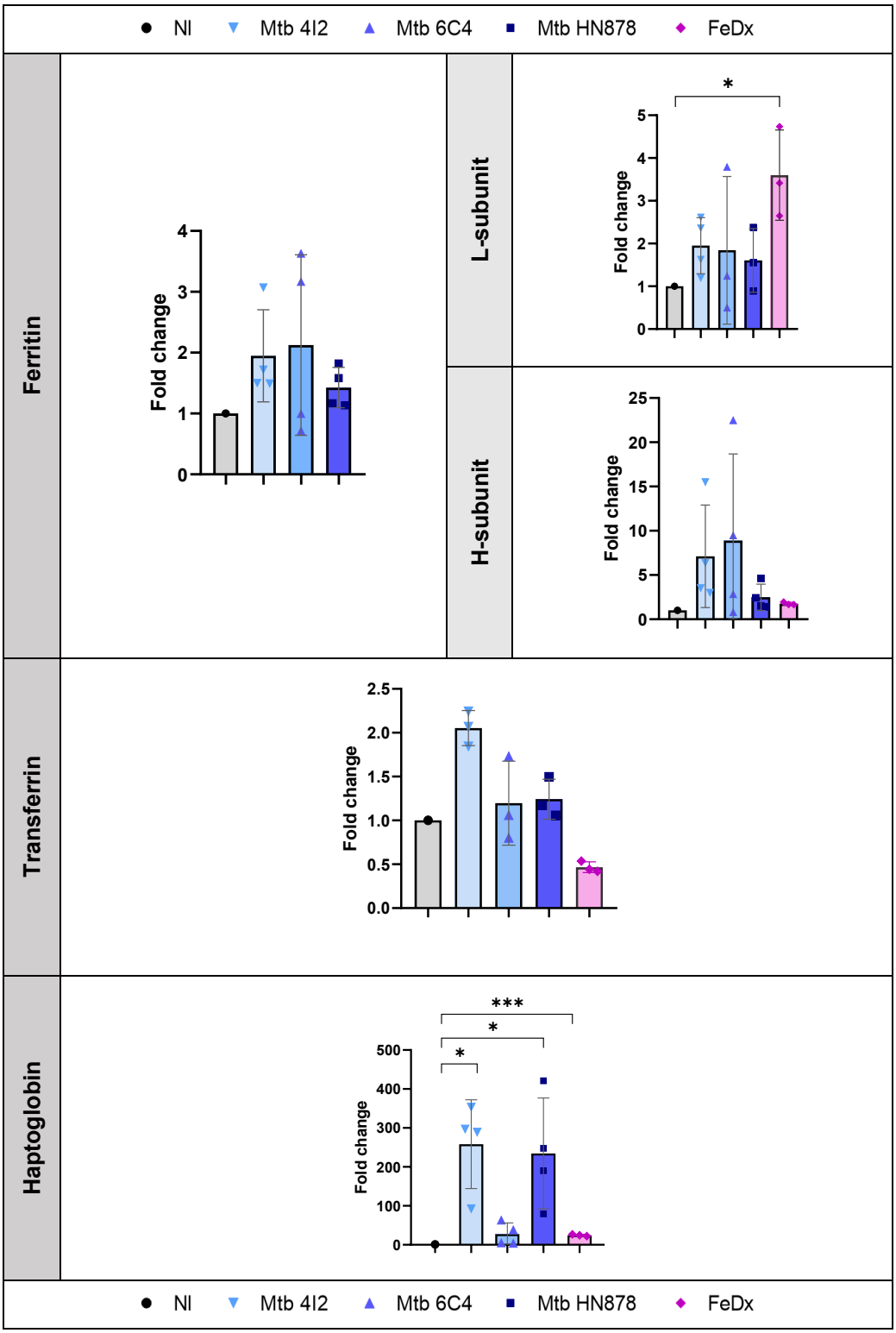

Figure 6 – *Quantification of iron-related proteins in the serum of mice infected with M. tuberculosis or iron overloaded.* C57BL/6 mice were either infected with strains of *M. tuberculosis* of different virulences or received a single dose of iron dextran (FeDx) to induce iron overload. The concentrations of ferritin (and its L- and H-subunit), transferrin and haptoglobin were determined in the mice sera by ELISA. Results are reported as fold change: infected mice relative to non-infected controls, and iron-overloaded mice relative to dextran-treated controls. Bars represent the mean, and the symbols represent individual values of 3 to 4 animals per group. Statistics: ordinary one-way ANOVA * $p < 0.05$, *** $p < 0.001$.

As shown in Figure 6, serum FT levels increased, both in response to *M. tuberculosis* infection and to iron overload. Unfortunately, it was not possible to measure FT with the commercial ELISA in the iron-overloaded mice due to time constraints. When the levels of each of the FT chains, H and L, were quantified separately, clearly different patterns were observed. Upon infection, serum FTH levels increased 3 to 7-fold, while FTL increased less than 2-fold. The opposite was seen in iron overload: FTH increased about 2-fold and FTL increased about 4-fold. Interestingly, in the case of Mtb-infected mice, the increase of FT levels was not correlated with the severity of the different strains evaluated.

These results are in accordance with what was previously reported by our group and others: circulating FTH levels increase during a mycobacterial infection [49]. FTH and FTL are both upregulated during inflammation, but FTH is more sensitive to inflammatory stimuli [72], while FTL responds predominantly to iron levels [73].

TF levels did not follow a consistent trend during *M. tuberculosis* infection. In mice infected with the mild strain, TF levels showed a 2-fold increasing trend, whereas those infected with more virulent strains showed no significant change. However, reports in humans indicate that circulating TF levels typically decrease during mycobacterial infection, [52] aligning with the expected host iron-withholding mechanisms [74]. Under iron overload conditions, TF levels were non-significantly reduced.

Finally, haptoglobin levels increased across all the experimental conditions tested. The increase was more pronounced in *M. tuberculosis*-infected mice compared with mice under iron overload. As an acute-phase protein, haptoglobin levels typically rise in an inflammatory context, such as the one seen in TB [75, 76]. In the iron overload model, the elevated haptoglobin levels were likely a consequence of the high circulating iron levels, which triggered an acute-phase inflammatory response in the mice. This response, occurring within 24 hours of FeDx injection, would have stimulated hepatic haptoglobin synthesis [77].

2. Iron metabolism proteins as predictors of TB disease progression in humans

Plasma proteomics has emerged as a powerful tool for the discovery of diagnostic biomarkers in TB, offering a comprehensive overview of systemic protein alterations that reflect host-pathogen interactions [52]. Proteomic profiling allows simultaneous detection

and quantification of hundreds of plasma proteins. These data provide insights into metabolic changes, immune responses, and dysregulated pathways associated with TB progression [60]. Iron metabolism is a critical element in TB pathology, as *M. tuberculosis* depends on host iron for survival. For that reason, the host immune system engages in iron sequestration as part of nutritional immunity. Thus, in the present analysis, special attention was given to iron-related proteins in plasma samples from healthy individuals, subjects with TB infection (TBI), and patients with TB disease (TBD). Evaluation of the abundance and regulation of iron-binding and iron-transport proteins aimed to identify group-specific expression patterns. Such patterns may be useful to assess potential diagnostic biomarkers, offering the ability to discriminate not only between TB cases and healthy controls but also between infection and disease.

2.1. TB cohort characterization

For this study, the plasma of 27 individuals with TB disease (TBD), 47 individuals with TB infection (TBI) but no disease, and 18 healthy controls (Control) was analysed. The characteristics of the study participants are described in Table 2.

Table 2 - *Demographic and clinical characteristics of the study participants*

Characteristic	**TB disease** N = 27[1]	**TB infection** N = 47[1]	**IGRA negative controls** N = 18[1]	**Overall** N = 92[1]	**p-value**[2]
Age, y, median (range)	40 (21–77)	34 (20–76)	41 (23–70)	35 (20–77)	0.300
Females, n (%)	17 (63%)	24 (51%)	6 (33%)	47 (51%)	0.200
Region of origin					0.300
Africa	9 (33%)	16 (34%)	2 (11%)	27 (29%)	—
Asia	8 (30%)	19 (40%)	3 (17%)	30 (33%)	—
Europe	7 (26%)	3 (6.4%)	3 (17%)	13 (14%)	—
N/A	2 (7.4%)	7 (15%)	9 (50%)	18 (20%)	—
South America	1 (3.7%)	2 (4.3%)	1 (5.6%)	4 (4.3%)	—
IGRA results					<0.001
Positive	20 (74%)	40 (85%)	0 (0%)	60 (65%)	—
Negative	2 (7.4%)	0 (0%)	18 (100%)	20 (22%)	—
N/A	5 (19%)	7 (15%)	0 (0%)	12 (13%)	—

Characteristic	TB disease N = 27[1]	TB infection N = 47[1]	IGRA negative controls N = 18[1]	Overall N = 92[1]	p-value[2]
Smear results (microscopy)					—
Positive	5 (19%)	0 (0%)	—	5 (6.8%)	—
Negative	15 (56%)	7 (15%)	—	22 (29.7%)	—
N/A	7 (26%)	40 (85%)	—	47 (63.5%)	—
Molecular results (PCR)					—
Positive	6 (22%)	0 (0%)	—	6 (8.1%)	—
Negative	13 (48%)	0 (0%)	—	13 (17.6%)	—
N/A	8 (30%)	47 (100%)	—	55 (74.3%)	—
Mtb culture, n (%)					—
Positive	21 (78%)	0 (0%)	—	21 (28.4%)	—
Negative	2 (7.4%)	0 (0%)	—	2 (2.7%)	—
N/A	4 (15%)	47 (100%)	—	51 (68.9%)	—
Any comorbidity, n (%)	12 (44.4%)	16 (34%)	3 (16.7%)	31 (33.7%)	—
CRP (mg/L, ref < 3)	5 [1, 19]	2 [1, 4]	1 [1, 1]	2 [1, 7]	0.006
ESR (mm, ref < 20)	35 [14, 77]	16 [7, 30]	18 [13, 23]	19 [10, 36]	0.030
WBC (10^9/L, ref 4.4-10.0)	6.30 [5.50, 7.50]	5.90 [4.80, 8.30]	6.05 [5.50, 6.60]	6.15 [5.10, 7.70]	0.600
HB (g/L, ref >120(F)/>130(M))	130 [115, 136]	137 [127, 149]	138 [133, 142]	135 [125, 145]	0.100
ALB (g/L, ref >38)	35.5 [31.0, 39.0]	39.5 [37.0, 42.0]	41.0 [41.0, 41.0]	38.0 [35.0, 41.0]	0.030

[1]Median (Min–Max); n (%); Median [Q1, Q3]

[2]Kruskal-Wallis rank sum test

Notes: Continuous variables shown as median (range) or median [IQR]. P values from Kruskal–Wallis (continuous) and Fisher's exact or chi-square with Monte Carlo (categorical), excluding 'N/A' levels from testing.

Abbreviations: IGRA = interferon-gamma release assay; PCR = polymerase chain reaction; WBC = white blood cells; HB = hemoglobin; ALB = albumin.

In line with Sweden's low TB incidence, most study participants were foreign-born, predominantly from Africa and Asia (Table 2). For TBD cases, blood samples were obtained within one week of initiating anti-TB therapy. Significant comorbidities were uncommon, and 1 participant in the TBD group was receiving immunosuppressive treatment. All TBD patients tested negative for HIV, while participants with TB infection and healthy controls were not routinely screened for HIV.

Table 2 also shows that, regarding both age and sex, all groups had a similar distribution. Still, the TBI patients were somewhat younger than the healthy controls and the TBD groups, whereas the healthy controls had a higher proportion of male participants. Still, the cohort's demographic profile was representative of the global TB burden [3]. The sex distribution was nearly balanced, consistent with the 2023 WHO Global TB Report [3], which indicates that men accounted for 55% of worldwide cases. Age distribution was also in line with global trends, with most participants falling within the adult age groups in which TB incidence is highest [3].

2.2. Protein Filtering - Iron-related proteins

The plasma from the previously described individuals was analysed for the differential abundance of more than 5400 proteins, using the Olink Explore HT Proximity Extension Assay. Members from the Human Protein Atlas (HPA) program, at SciLifeLab, excluded one sample based on outlier detection. After quality control, an additional four samples were removed from further analysis. These samples showed atypical expression patterns, and since they represented different subcategories (two healthy controls, one TBI, and one TBD), their profiles were considered unlikely to have a biological reason. Finally, 87 samples were included in the complete study.

As previously described, the proteomics assay used can detect more than 5400 proteins. To narrow the analysis to iron-related proteins, the dataset was filtered based on a curated list of 21 relevant proteins (Table 3). These proteins were chosen based on previous knowledge of their role in iron metabolism and/or relevance for TB infection outcome and host immune-related response. Only these proteins were included in the subsequent analyses.

Table 3 – *Relevant proteins under analysis.* These proteins were chosen based on previous knowledge of their role in iron metabolism and/or relevance for TB infection outcome and host immune-related response

Protein	Gene name	Function
C-C motif chemokine 2	*CCL2*	Pro-inflammatory chemokine [78]
C-X-C motif chemokine 10	*CXCL10*	Recruitment of immune cells, induced by IFNG [79]
Interferon γ	*IFNG*	Activates macrophages, coordinates immune defense against pathogens [80]
Interleukin-1 β	*IL1B*	Pro-inflammatory mediator [81]
Interleukin-6	*IL6*	Cytokine involved in inflammation, acute phase response [82]
Interleukin-10	*IL10*	Anti-inflammatory cytokine [83]
Interleukin-12 subunit β	*IL12B*	Forms part of IL-12 and IL-23, driving Th1 cell differentiation and IFNG production [84]
Interleukin-18	*IL18*	Promotes IFNG production, enhancing Th1 immune responses [85]
Tumor necrosis factor	*TNF*	Central mediator of inflammation; it induces cell death and activates immune responses [86]
Interferon γ receptor 1	*IFNGR1*	Binds IFNG to initiate immune signaling [87]
Interferon γ receptor 2	*IFNGR2*	Works with IFNGR1 to transduce IFNG signals inside the cell [87]
Bone morphogenetic protein 6	*BMP6*	Stimulates hepcidin production [88]
Hemojuvelin	*HJV*	Regulator of hepcidin production [89]
Heme oxygenase 1	*HMOX1*	Heme degradation [90]
Hephaestin	*HEPH*	Ferroxidase - oxidizes Fe^{2+} to Fe^{3+}, enabling transferrin binding for export [91]
Ferritin light chain	*FTL*	Stores excess intracellular iron in a non-toxic form [27]
Lactotransferrin	*LTF*	Sequesters iron to inhibit bacterial growth [92]
Serotransferrin	*TF*	Binds and transports Fe^{3+} in the blood to cells [23]
Transferrin receptor protein 1	*TFRC*	Mediates cellular uptake of transferrin-bound iron [24]
Solute carrier family 40 member 1	*SLC40A1*	(Ferroportin) Iron transporter [93]
Transcription regulator protein BACH1	*BACH1*	Represses genes involved in antioxidant defense and heme/iron metabolism [94]

Unfortunately, despite the extremely high number of proteins under analysis in the HT Explore Olink Protein Extension Assay, some important iron-associated proteins, such as FTH and haptoglobin, were not included in the panel, restricting the analysis to

the set of proteins in Table 3. The filtered proteins included cytokines, closely associated with the immune response triggered by a mycobacterial infection, besides being involved in iron regulation, such as TNF, IFNG and IL6, or proteins directly involved in iron metabolism, including TF, FTL and SLC40A1. A brief description of each protein's function under analysis is presented in Table 3. Regarding the transferrin receptor protein 1 (TFR1), we were unable to clarify whether the measured signal corresponded to the full-length protein or to its cleaved, soluble form, usually found in circulation. For consistency and simplicity, the protein is referred to as TFR1 throughout the text, while the gene designation, *TFRC*, used by the company that performed the measurements, is kept in the figures.

2.3. Exploratory data analysis

To get an overview of the distribution of the abundance of each iron-associated protein across different stages of TB, a heatmap illustrating the expression levels of the selected proteins was created (Figure 7).

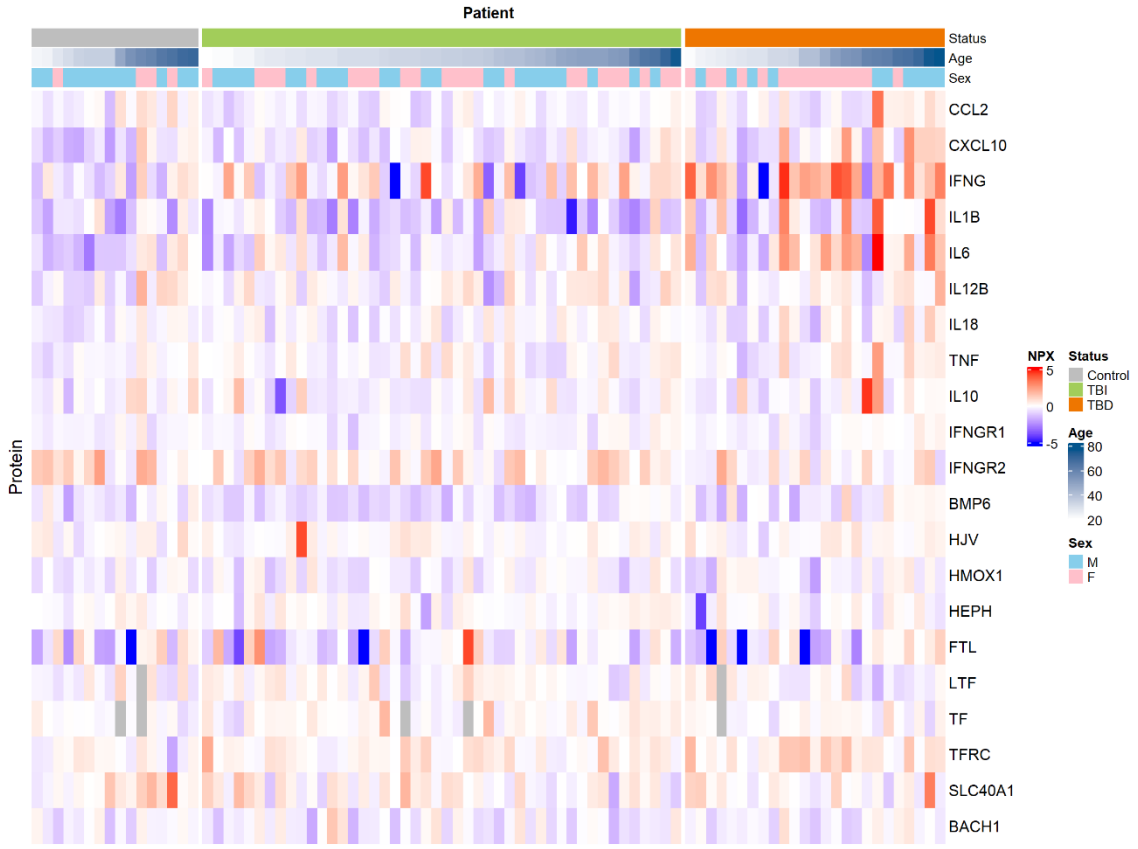

Figure 7 – *Heatmap of iron-related protein abundance across the tuberculosis (TB) cohort.* Samples are ordered by clinical status (controls, TBI (TB infection), and TBD (TB disease)), and, within each status, by age. Signals are shown as NPX (Normalized Protein eXpression), a relative-abundance metric. Sex is annotated per sample.

Overall, the heatmap analysis revealed no consistent expression patterns across the different clinical conditions assessed. This finding was noteworthy given the existence of several studies reporting differential circulating levels of some of these proteins [52]. However, there appeared to be a difference in IFNG and IL6 expression patterns between the control and TBD groups.

These preliminary results obtained through the heatmap interpretation were confirmed by a Principal Component Analysis (PCA) (Figure 8). PCA is a widely used technique for linear dimensionality reduction, which simplifies high-dimensional data by reducing it into lower dimensions while maintaining as much of the original data's variability as possible. These lower-dimensional representations enhance the comprehension of the data, with two-dimensional PCA plots frequently used in exploratory analysis to reveal patterns and outliers [95]. PCA translates into finding new variables that are linear functions of those in the original dataset, that successively maximize variance, and that are uncorrelated with each other [96].

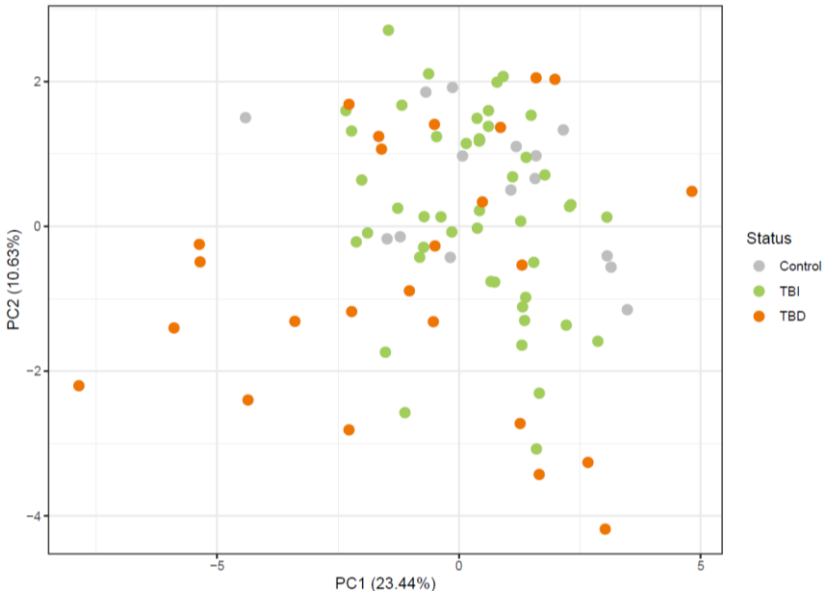

Figure 8 - *Principal component analysis (PCA) of iron-related protein profiles across the tuberculosis cohort.* Each point represents one participant; colors represent clinical status: Control (grey), TBI – TB infection (green), and TBD - TB disease (orange). Axes show the first two principal components, explaining 23.44% (PC1) and 10.63% (PC2) of the total variance. Positions were obtained from NPX (Normalized Protein eXpression) values.

In the PCA plot shown in Figure 8, the distribution of data points (samples) indicated that the 21 selected proteins did not differentiate the sample groups, as no distinct clustering or separation was observed. Ideally, meaningful groupings would appear as well-defined clusters. Furthermore, the variance explained by the first few principal components was relatively low, suggesting that these components do not capture a considerable portion of the total data variability.

2.4. Evaluation of protein patterns according to TB severity

Considering the lack of differences among the previously established groups, we hypothesized that differences could become apparent if we analysed different severity states, within the TBD group. For that purpose, a 12-protein signature associated with TB severity, previously determined and published by *Mousavian et al.* [97] (Table 4), was used to define the groups. PCA was performed to cluster TBD into two subgroups: non-severe and severe TBD (Figure 9).

Table 4 - *12-protein signature associated with TB severity determined by Mousavian et al. (2022)*

Protein	Gene name
Interferon gamma	IFNG
Interleukin-6	IL6
CUB domain-containing protein 1	CDCP1
Interleukin-7	IL7
Interleukin-12 beta	IL12B
C-X-C motif chemokine 9	CXCL9
Interstitial collagenase	MMP1
C-C motif chemokine 7 (CCL7)	MCP3
C-C motif chemokine 19	CCL19
TNF receptor superfamily member 5	CD40
Vascular endothelial growth factor A	VEGFA
Programmed cell death 1 ligand 1 (PD-L1)	CD274

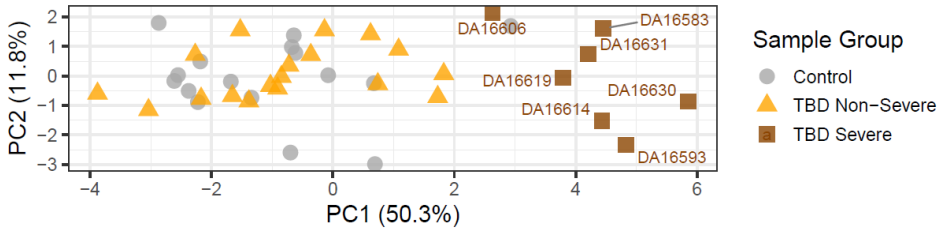

Figure 9 - *Principal component analysis (PCA) of a 12-protein tuberculosis (TB) severity signature.* PCA was performed on NPX values for a curated 12-protein panel previously associated with disease severity. Each point is one participant; shapes represent groups: Control (grey circles), TBD Non-Severe (gold triangles), and TBD Severe (brown squares; sample IDs shown). The first two components explain 50.3% (PC1) and 11.8% (PC2) of the variance.

Following PCA, two distinct subgroups were formed. Classification of these as “non-severe” or “severe” was determined by comparison with the PCA distribution of the control group, with the subgroup most closely aligned with the control profile designated

as non-severe. Severe TBD samples cluster at higher PC1 scores, indicating a distinct global profile of the severity-associated proteins, whereas Controls and Non-Severe cases largely overlap at lower PC1. PC2 captures additional within-group dispersion. These results were in line with the ones obtained by the same type of PCA analysis for the iron-related proteins previously chosen in Table 3 (Figure 10).

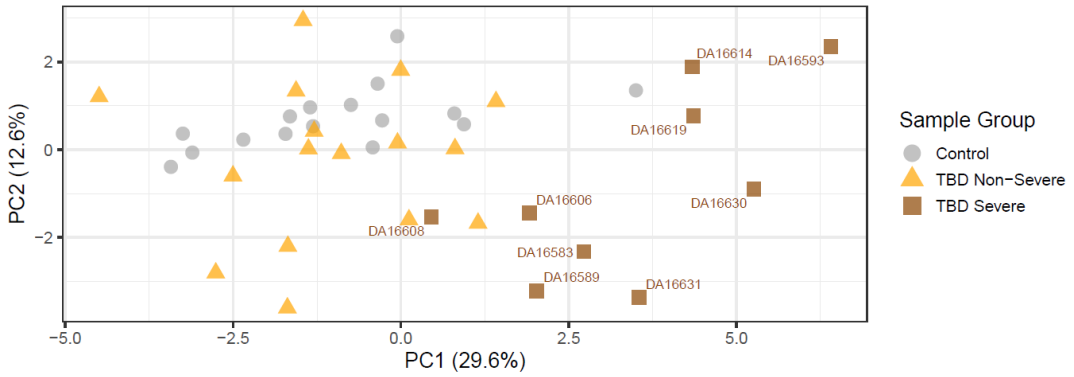

Figure 10 - *Principal component analysis (PCA) of a 21-protein iron-related panel in the tuberculosis cohort.* PCA was performed on NPX values for 21 proteins involved in iron homeostasis. Points represent individual participants; symbols indicate groups: Control (grey circles), TBD Non-Severe (gold triangles), and TBD Severe (brown squares; sample IDs annotated). The first two components explain 29.6% (PC1) and 12.6% (PC2) of the total variance.

In both the PCA based on the 12-protein signature associated with TB severity (Figure 9) and the PCA based on the iron-related proteins panel (Figure 10), the TBD group was separated into two distinct clusters in a similar manner. Comparison of sample identities revealed seven individuals common to the same cluster in both analyses. The overlapping samples were consequently classified as “severe”, supporting the potential of the iron-related proteins as indicators for TB severity.

To further validate the PCA-derived TBD subgroups, biochemical markers indicating more extensive inflammation, such as lower hemoglobin (HB) and albumin (ALB), and higher erythrocyte sedimentation rate (ESR) and C-reactive protein (CRP), obtained from the patients' clinical records, were analysed (Figure 11).

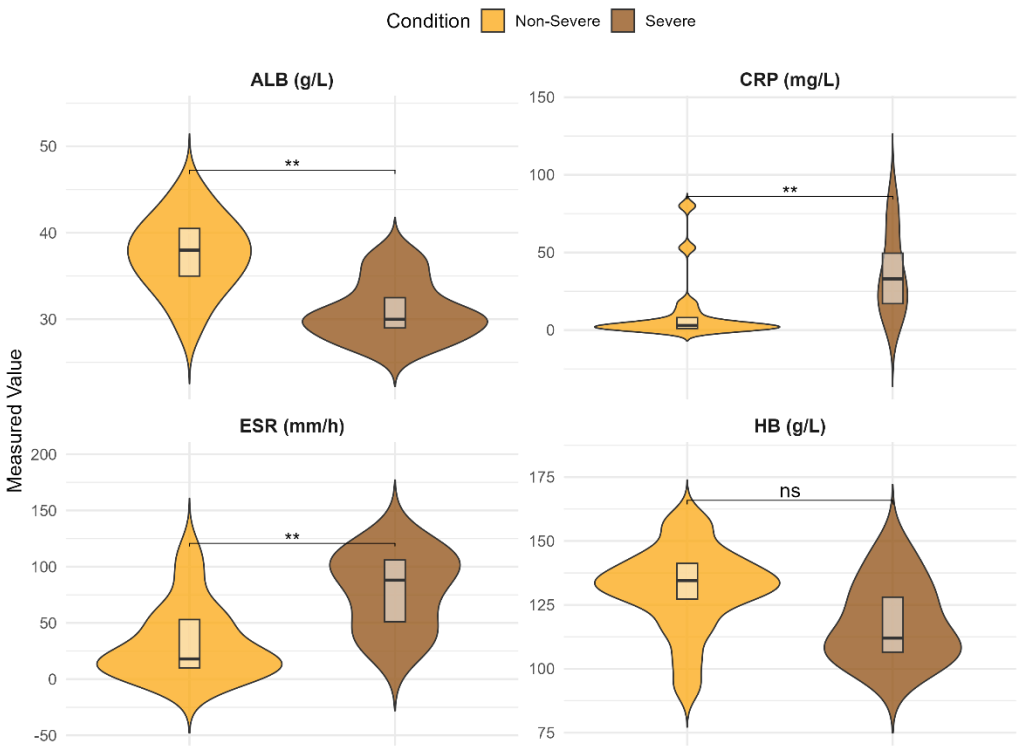

Figure 11 - *Systemic inflammatory markers by tuberculosis (TB) disease severity.* Violin plots show the distribution of (A) serum albumin (ALB, g/L), (B) C-reactive protein (CRP, mg/L), (C) erythrocyte sedimentation rate (ESR, mm/h), and (D) hemoglobin (HB, g/L) in TBD Non-Severe (gold) and TBD Severe (brown) groups. The central line represents the median and the white box the interquartile range. Statistics: unpaired t-test, ** $p < 0.01$.

The blood biochemistry-related parameters supported the TBD subdivision formed by PCA. Consistent with clinical manifestations of disease, patients with severe TBD exhibited significantly higher CRP and ESR levels, along with lower ALB and a tendency for lower HB levels, compared with non-severe TB patients (Figure 11).

2.5. Differentially abundant proteins determination

After refining the analysis according to the TBD severity, a differentially abundant protein analysis of the Olink Explore HT Proximity Extension Assay data was performed (Figure 12). This analysis was conducted to identify proteins capable of discriminating between the defined cohort subgroups, with an emphasis on the iron-related proteins previously chosen.

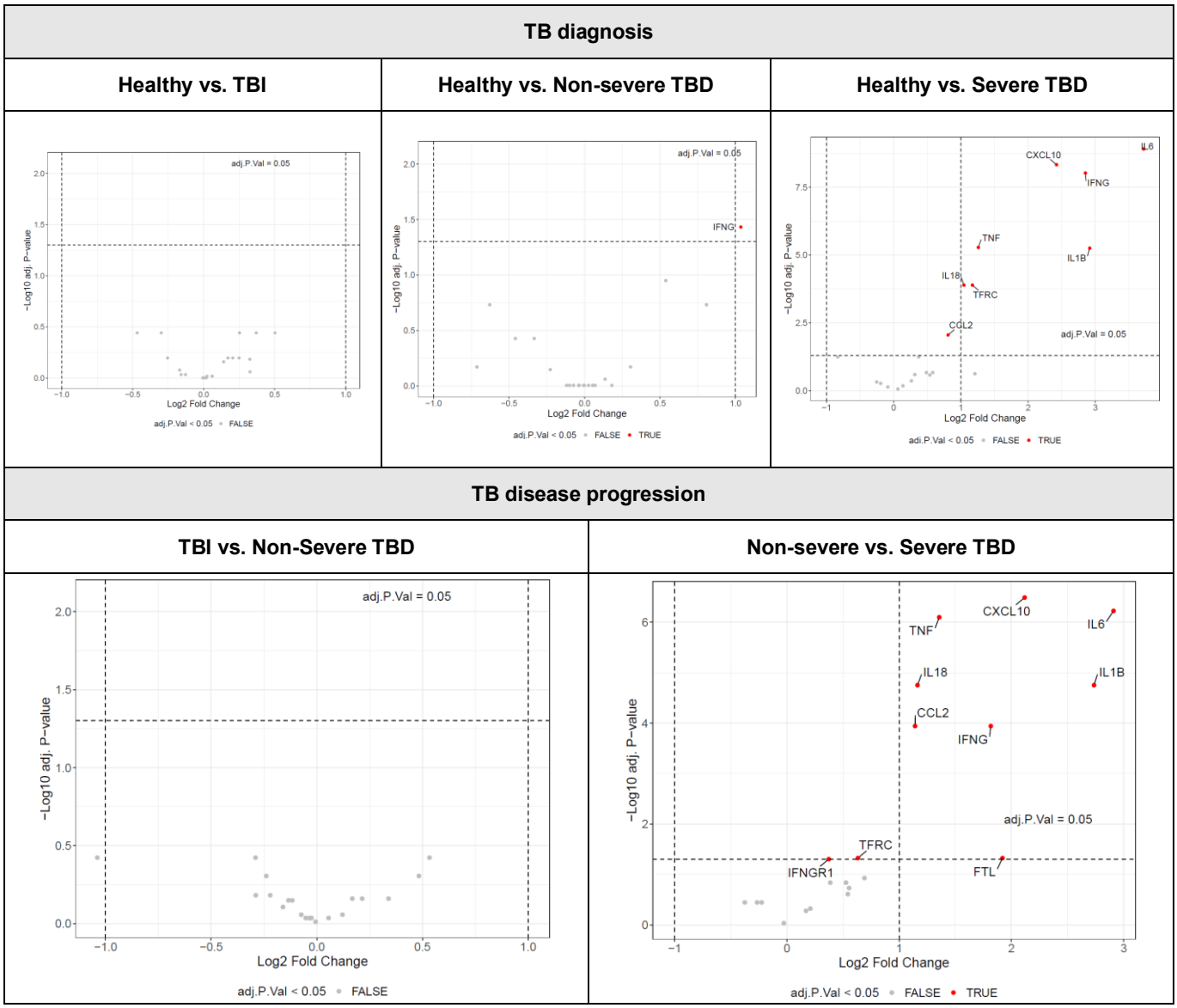

Figure 12 – *Differential abundance analysis for TB diagnosis and disease progression*. Volcano plots show $\log_2$ fold change vs. $-\log_{10}$ adjusted P value (y-axis) for each iron-related protein. Top row: diagnostic comparisons (Healthy vs. TBI, Healthy vs. Non-severe TBD, Healthy vs. Severe TBD). Bottom row: progression comparisons (TBI vs. Non-severe TBD, Non-severe vs. Severe TBD). The horizontal dashed line marks the FDR threshold (adjusted P = 0.05); vertical dashed lines indicate the effect-size cutoff used for annotation. Points in red are significant proteins.

Differential protein abundance analysis compares protein expression levels between predefined groups to identify statistically significant differences. In this study, two analyses were performed: one to identify potential iron-related diagnostic biomarkers and another to explore iron-related protein signatures associated with TB disease progression. Proteins meeting predefined thresholds for fold-change and adjusted *p*-value were considered differentially abundant, namely those with an adjusted p-value < 0.05 and an absolute $\log_2$ fold-change greater than 1. This approach allowed the

identification of proteins whose expression patterns are associated with TB disease severity, highlighting candidates of potential diagnostic relevance.

In the diagnostic comparisons, the healthy control group was tested independently against each TB condition to detect proteins uniquely associated with different disease states (Figure 12, top panels). No significant protein changes were detected between healthy controls and individuals with TBI or non-severe TBD. By contrast, severe TB exhibited a broad upregulation of proteins, including inflammatory mediators (e.g., CXCL10, IFNG, TNF), as well as immunity/iron-handling factors (e.g., TFR1, CCL2, IL1B), with no comparably significant downregulation. These results indicate that the strongest remodeling of the circulating proteome occurs in severe disease. The set of proteins chosen for this analysis mainly discriminated between the healthy controls and the most severe TBD patients, and, within those significantly distinct proteins, only TFR1 was directly related to iron metabolism. The remaining differentially abundant proteins, namely IFNG, TNF, IL6, IL18, CCL2 and CXCL10, revealed a significant increase in abundance, a finding that was anticipated based on their well-established roles in the immune response.

In the progression-focused analysis, no significant differences were observed between TBI and non-severe TB disease (Figure 12, bottom left). However, comparison of non-severe with severe TB identified a distinct set of differentially expressed proteins (Figure 12, bottom right). Severe TB was characterized by strong upregulation of pro-inflammatory mediators (IL6, IL1B, TNF, IFNG, CXCL10, CCL2, and IL18), alongside significant changes in iron-related proteins. Specifically, TFR1 was modestly upregulated, indicating increased cellular iron demand, while FTL was elevated, consistent with enhanced intracellular iron sequestration during an advanced disease stage.

2.6. Iron-related proteins abundance (with TBD subgroups)

To assess whether the iron-related proteins could be used to discriminate between different TB disease stages, the relative abundance of each protein was compared across healthy controls, individuals with TB infection, and patients with less or more severe disease (Figure 13). This analysis aimed to identify proteins whose expression patterns change consistently with disease progression, thereby highlighting potential stage-specific biomarkers.

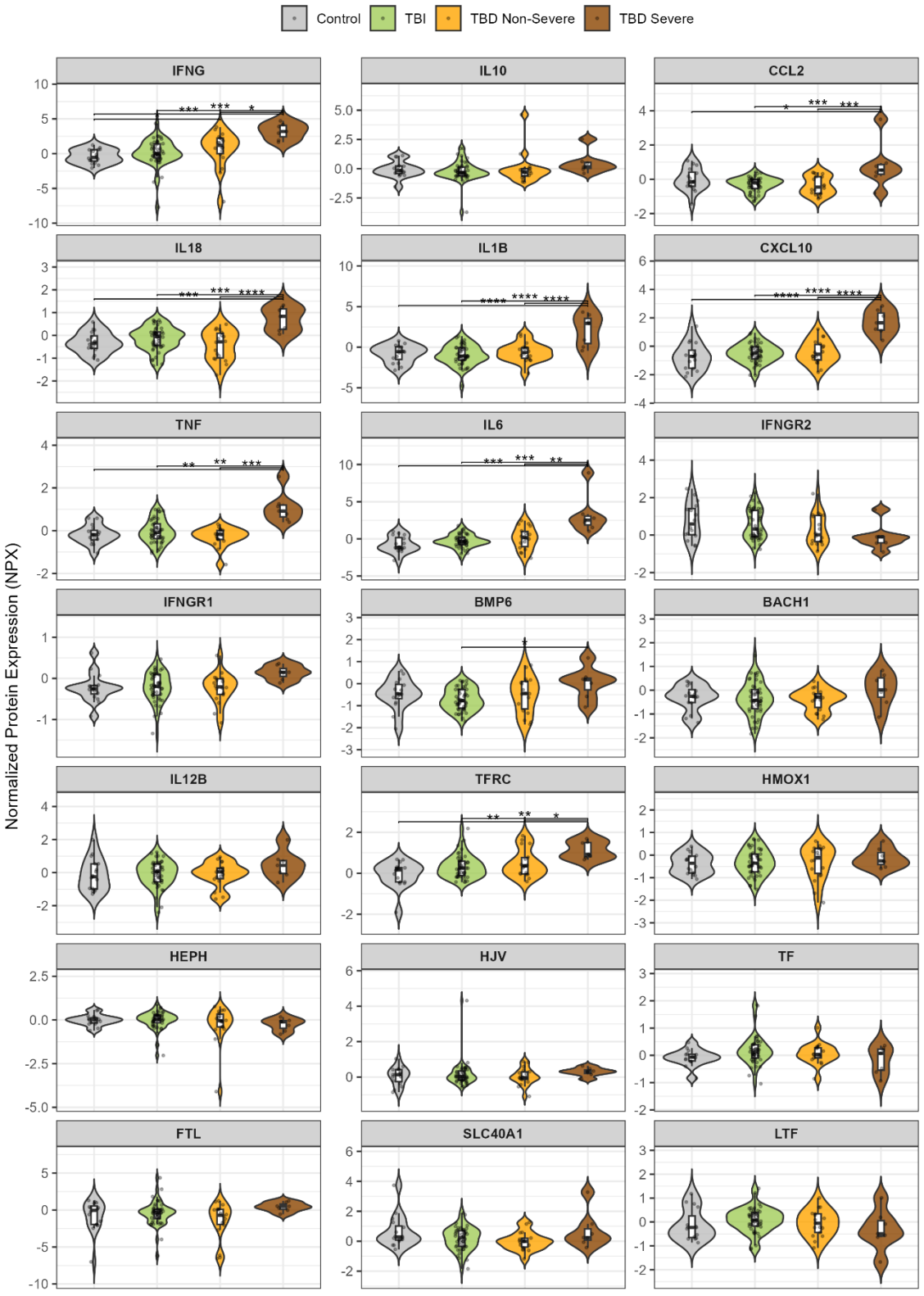

Figure 13 - *Distribution of iron-related and inflammatory proteins by tuberculosis (TB) status.* Violin plots show Normalized Protein eXpression (NPX, relative abundance) for the 21-protein panel across Control (grey), TBI (light green), TBD Non-Severe (gold), and TBD Severe (brown) groups. Within each violin, the white box marks the interquartile range and the horizontal line the median. Statistics: NPX by group with significance bars – ANOVA + Tukey when assumptions met, else Kruskal–Wallis + Wilcoxon (BH-adjusted), * $p < 0.05$, ** $p < 0.01$, *** $p < 0.001$, **** $p < 0.0001$.

As shown in Figure 13, cytokines involved in the immune response to *M. tuberculosis* infection, such as TNF and IL6, were significantly elevated in patients with a more severe TB disease when compared with healthy controls. In contrast, IL10, an anti-inflammatory cytokine, did not change substantially between groups, suggesting that regulatory immune mechanisms are not proportionally activated in severe disease.

When focusing on iron-related proteins, a more restricted pattern was observed. The transferrin receptor TFR1 was significantly elevated in severe TB compared with non-severe disease and controls, consistent with increased cellular iron demand in advanced disease. FTL also showed higher levels in severe TB, although the differences were more modest. For other iron-related proteins (BMP6, HJV, HMOX1, TF, SLC40A1, LTF), expression patterns were variable and did not consistently distinguish disease groups, suggesting limited interpretability in the studied dataset. Taken together, these results confirm that inflammatory proteins were the most robust indicators of TB status, while among iron-related proteins, only TFRC and FTL showed the clearest associations with disease severity, supporting the results previously obtained in the differential protein abundance analysis (Figure 12).

Given ferritin's central role in iron homeostasis and its potential relevance as a disease biomarker, an additional targeted analysis was performed to quantify ferritin across the cohort (Figure 14). This approach aimed to determine whether ferritin abundance could serve as an indicator of TB disease progression.

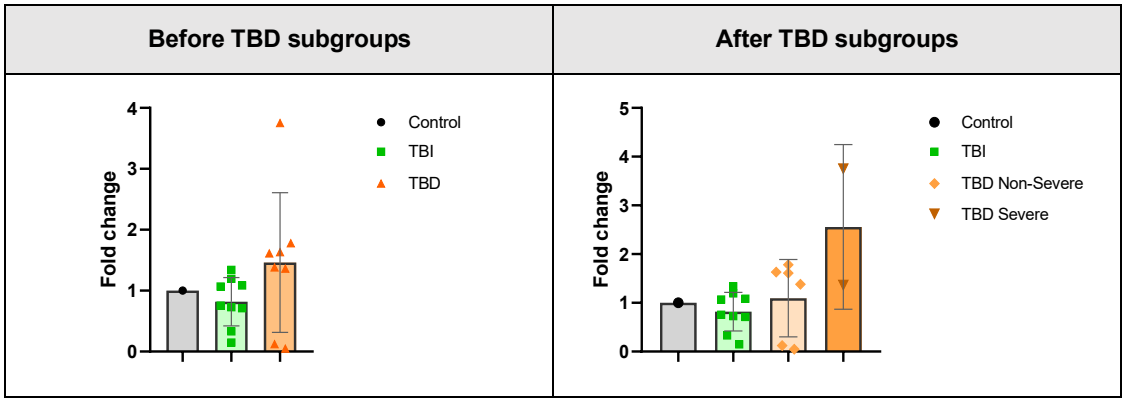

Figure 14 – *Circulating ferritin levels before and after stratifying TB disease (TBD) by severity.* The y-axis shows fold change relative to the Control group mean. Left: groups aggregated as Control (black circles), TBI (green squares), and all TBD (orange triangles). Right**:** TBD split into Non-Severe (orange diamonds) and Severe (orange inverted triangles), with Controls and TBI shown for reference. Bars represent the mean, and the symbols represent the participants' individual values. Statistics: ordinary one-way ANOVA.

Analysis of Figure 14 demonstrates that FT levels were higher in patients with TB disease, as expected. This difference became more apparent when applying the TBD subgroup classification, despite the limited sample size in the severe TBD group. The

analysis suggested that FT may help differentiate between healthy individuals or patients with TBI and those with severe TBD. However, it did not discriminate effectively between healthy individuals, TBI patients, and those with non-severe TBD, as no significant differences were observed among these groups. These findings differ from those reported by Dai *et al.* [52], who observed significant differences in FT levels between TBI and TBD patients. However, similar to our results, they found no evidence that FT could distinguish healthy individuals from those with TBI, highlighting the limitations of FT as a biomarker for confirming the absence of infection.

Discussion

Mycobacteria are intramacrophagic pathogens, therefore, when infection occurs, they must compete against the host for iron availability [98]. Mammals have developed a set of immunological mechanisms to sequester and withhold bioavailable iron, resulting in iron redistribution [27, 40]. Efforts have been made to understand how iron homeostasis is altered within various parts of the host, including in the bloodstream [52]. The role of circulating iron-related proteins has also been gathering interest [52, 99]. These studies have identified several changes in key regulators of iron homeostasis, such as increased levels of FTH, the catalytic subunit of the primary iron storage protein, in specific tissues and its presence in circulation [49]. However, these variations in FT levels are not exclusive and are not clearly indicative of TB [100]. The need to explore additional iron-related proteomic changes emerges from the objective of identifying TB in a clinical setting and, ultimately, distinguishing between its different disease stages.

In this work, we first examined the alterations in circulating iron metabolism proteins induced by *M. tuberculosis* infection and by iron overload in a mouse model (Figure 6). High levels of iron usually facilitate pathogen proliferation and accelerate disease progression, while iron chelation can effectively restrict microbial growth [101, 102]. In response, the host adopts a range of defense strategies aimed at depleting circulating iron, thereby limiting its use by mycobacteria [103]. Among the molecules implicated in this iron-sequestering response, FTH may play a contributory role. In fact, *Reddy et al.* [104] provided evidence that FTH plays a critical role in protecting mice against *M. tuberculosis* infection by participating in several key processes, such as maintenance of mitochondrial function [58]. The distinct regulation of FTH and FTL reflects their specialized roles in iron metabolism and the inflammatory response - specifically, the differential regulation of the two ferritin subunits in response to distinct stimuli [33, 105]. Our results confirmed that FTH showed greater sensitivity to inflammatory stimuli, while FTL responded predominantly to elevated iron levels (Figure 6). In summary, the differential expression of FTH and FTL suggests that ferritin subunit profiling may serve as a useful biomarker to distinguish mycobacterial infection from other causes of hyperferritinemia, thereby improving diagnostic accuracy and guiding appropriate management. However, this analysis was conducted in a small number of mice, limiting the power of the findings. FTL levels were significantly elevated in iron-overloaded mice compared with controls, while no statistical differences were observed for FTH. This might indicate that FTL is more sensitive to alterations in systemic iron status [106]. In addition, the assessment of total ferritin levels in the iron-overloaded group would have provided valuable complementary information. From a diagnostic perspective, evaluating the circulating FTL/FTH ratio remains of particular interest, but this requires further

investigation using larger sample sizes to reliably determine whether distinct ferritin subunit responses can be detected under different stimuli associated with hyperferritinemia.

Although no prior studies have extensively examined the effect of *M. tuberculosis* infection on circulating TF levels in mice, reports in humans indicate that circulating TF levels typically decrease during mycobacterial infection [52]. This response aligns with expected host iron-withholding mechanisms [74]. Regarding infection, our results were not consistent (Figure 6). In the mild *M. tuberculosis* strain, the levels showed unexpected increasing trends; this response was not observed in the other evaluated strains, and none of these differences reached statistical significance. Finally, as an acute-phase protein, haptoglobin levels typically rise in an inflammatory context, such as the one seen in TB [75, 76], which was clearly seen in our results (Figure 6), with a significant increase across all *M. tuberculosis* strains. However, this increase was also seen during iron overload. High levels of circulating iron are known to trigger a pro-inflammatory response, as seen in increasing circulating levels of IL-6 and TNF-α, both pro-inflammatory cytokines, as reported by Tsay, Yang [77]. However, in that study, the mice received substantially higher cumulative FeDx exposure administered over a two-month dosing regimen, limiting direct comparison with our conditions. For that reason, we did not find, in our study, transferrin and haptoglobin to be reliable circulating biomarkers for differentiating mycobacterial infection from other conditions that disrupt iron homeostasis. These findings highlight the need to identify additional iron-related protein candidates for TB diagnostics.

To address this, we performed a blind, data-driven bioinformatic analysis of plasma samples from a cohort of TB patients. The aim was to determine whether iron-metabolism-associated protein signatures (Table 3) could reflect disease stage and predict progression from infection to TB disease. This topic has previously been investigated by Dai et al., who demonstrated that a biomarker signature consisting of iron, transferrin, and ferritin could successfully distinguish infection from TB disease [52]. Similarly, Minchella et al. provided further evidence linking iron homeostasis to TB progression in household contacts of infectious cases. In their cohort, progression to TB disease at any time point was associated with lower baseline concentrations of transferrin, while individuals who developed disease earlier exhibited higher baseline concentrations of ferritin and hepcidin compared to those who progressed later [107]. These findings supported the hypothesis that iron plays a functional role in TB pathogenesis and highlight the importance of iron-regulatory pathways in shaping host

susceptibility. Our initial exploratory analyses, including a heatmap (Figure 7) and PCA (Figure 8), did not reveal a clear separation between the study groups. In fact, the similarity in protein profiles among control, TBI, and TBD participants suggested that the individuals included in the study may not have reached a stage of illness severe enough to induce distinct expression changes. Consequently, we stratified the TBD group into subgroups of lower and higher severity (Non-severe and Severe TBD), using a well-established protein signature associated with TB disease (Table 4). With this refinement, the selected iron-related proteins successfully distinguished patients according to TBD severity (Figure 8), with overlapping results when compared to the 12-protein signature associated with TB severity (Figure 9). The overlaying PCA signatures of both healthy and Non-severe TBD patients were also a strong indicator of the less severe state of disease between these patients (Figure 9).

To corroborate the PCA-defined TBD subgroups, we next assessed biochemical markers reflective of systemic inflammation, characterized by decreased hemoglobin (HB) and albumin (ALB) concentrations, alongside increased erythrocyte sedimentation rate (ESR) and C-reactive protein (CRP) levels (Figure 11). The analysed biochemical markers reflected disease severity, as reported previously by Mousavian *et al.* [97]. CRP is an acute-phase protein that rises in response to infection or inflammation and, accordingly, is elevated in TB [108, 109]. The ESR is likewise increased in several inflammatory conditions, including TB. This increase reflects the infection-induced release of acute-phase proteins into circulation, promoting erythrocyte aggregation and accelerating sedimentation [110, 111]. TB may also induce anemia, resulting in reduced hemoglobin levels, and hypoalbuminemia, set as decreased serum albumin concentrations. Both alterations are commonly linked to inflammation and may be used as markers of disease severity and prognosis.

In order to identify proteins with expression patterns that track TB disease diagnosis and progression, combined differential abundance (Figure 12) and distributional protein abundance (Figure 13) analysis were performed. By examining both diagnostic group comparisons and disease progression, we aimed to identify iron-related protein signatures that could serve as biomarkers of disease diagnosis and severity assessment. Across all analyses, a clear finding was the strong upregulation of inflammatory proteins in severe TB disease. Both the volcano and the violin plots highlighted the increased abundance of IL6, IL1B, TNF, IFNG, CXCL10, CCL2, and IL18, consistent with an enhanced Th1 pro-inflammatory response, driving granuloma formation, macrophage activation, and immune cell recruitment [112]. This observation aligns with previous

findings that severe TBD is characterized by dysregulated IFNG signaling, cytokine storm-like activity, and tissue damage, phenomena that contribute directly to disease pathology [113]. Notably, TNF, CXCL10, IL1B and IL18 levels were consistently higher in both non-severe and severe TBD groups, suggesting that these pathways may be activated early in disease progression and further amplified with severity. As an anti-inflammatory cytokine, IL10 expression was moderately elevated in severe TBD, potentially reflecting the start of a compensatory response to enhanced pro-inflammatory activation [83]. This supports the idea that immune homeostasis in severe TBD involves the simultaneous activation of both pro- and anti-inflammatory pathways.

Among the iron-related proteins, the transferrin receptor protein 1 (TFR1) and ferritin light chain (FTL) were the most relevant iron-related proteins associated with TB severity. These findings were supported by the violin plot data, which confirmed higher TFR1 expression in severe TB compared with non-severe disease and controls, and suggested moderately increased FTL abundance. The biological implications of these findings are consistent with established models of iron metabolism in infection. TFR1 is responsible for mediating the uptake of TF-bound iron into cells [24]. During *M. tuberculosis* infection, TFR1 expression often increases as part of the host's physiological response to enhanced iron demand, particularly in rapidly dividing immune cells responding to the mycobacterial infection [114]. This reflects the host's attempt to sustain iron supply for the immune response. It was also previously shown that TFR1 mediates endocytic uptake of FTH, via a binding site distinct from the TF-binding site. In fact, erythroblasts that express high levels of TFR1 were able to incorporate FTH, whereas lymphocytes and granulocytes could not. This interaction becomes detectable only when the cell-surface TFR1 density exceeds a threshold [115, 116]. Minchella et al. previously reported elevated TFR1 levels during TB disease compared with both TST-positive and TST-negative contacts [117]. A critical aspect of our results would be to clarify whether the antibodies employed in the assay recognize an epitope common to both the cleaved and full TFR1 isoforms, or specific to the cleaved, soluble state. This uncertainty represents a limitation of the present results.

Increased FTL reflects sequestration of iron within macrophages, a host strategy designed to limit extracellular iron availability to the pathogen [106]. Similar observations have been reported by other groups. For example, macrophages have been shown to upregulate ferritin expression following *M. tuberculosis* infection [52]. A more recent study by Dai et al. demonstrated that both ferritin heavy chain (FTH) and FTL were significantly increased in macrophages containing live bacteria. It was also shown that

FTH1 knockdown was associated with enhanced intracellular growth of *M. tuberculosis*, supporting the importance of ferritin in restricting bacterial replication [118]. Another study reported that a significant decrease in ferritin concentrations was observed only after a six-month anti-TB treatment, highlighting its potential as a biomarker [119].

The observed increases in TFR1 and FTL together highlight the distinct processes of cellular iron need and host iron sequestration, while pointing towards a more severe inflammatory response. These iron sequestration processes are strongly linked to inflammation, particularly via IL-6-mediated induction of hepcidin, which reduces iron export from cells and favors intracellular storage [120]. Transferrin (TF) and ferroportin (SLC40A1), other studied iron-binding proteins, did not show consistent or significant clinical group differences. While linked to iron regulation, the variability here suggests that these proteins are less reliable as biomarkers in this dataset. Their expression may be more context-dependent, subtle, and influenced by factors not captured in this cohort. Further studies with larger sample sizes and functional assays will be needed to clarify their role.

These findings highlight two distinct but complementary signatures of severe TB. The first is an inflammatory signature, which is largely made up of cytokines and chemokines and appears to provide diagnostic discrimination between TB patients and controls. The second is an iron-related signature, best described by TFR1 and FTL, and perhaps more useful for the prediction of disease progression and severity. These signatures illustrate the complex interplay between host immune activation and iron regulation in TB. Clinically, these results suggest that inflammatory proteins are strong candidates for diagnostic biomarkers, but that adding iron-related proteins would be useful for classifying patients by risk of progression or severity. Overall, these results form the basis for future research on the use of panels of combined inflammatory and iron-related proteins as tools to manage TB. Given the results seen in the murine model, it would have been valuable to assess FTH levels in the present cohort. Incorporating this parameter into future, larger cohort studies will be essential to clarify its role in tuberculosis pathogenesis.

To complement the bioinformatic findings, we measured ferritin levels, which demonstrated promising potential for discriminating TB severity (Figure 14). Stratifying TB disease (TBD) by severity provided additional insight into host responses that were masked when TBD was analysed as a single group. Before subdivision, individuals with TBD showed higher fold changes compared to controls and TBI, but the wide variation was clear. After stratification, it became more clear that this increase was mostly driven

by patients with severe TBD while, in those with non-severe TBD, responses were closer to TBI. However, these results need to be interpreted with caution, as the severe TBD group included only two patients, limiting the generalization of this observation. These results highlight, once again, the need to differentially measure FTH in human sera or plasma.

Collectively, these findings suggest that the magnitude of host protein expression changes is directly related to disease severity. Severe TBD is characterized by exacerbated immune alterations, reflecting an uncontrolled infection, whereas non-severe TBD indicates a more restricted host-pathogen interaction. These differences underline the importance of considering disease heterogeneity when evaluating biomarkers. From a clinical standpoint, the ability to distinguish severe from non-severe disease has important implications. Biomarkers that increase proportionally with severity may allow early risk stratification, guide treatment intensity, and inform prognosis. Further, the overlap of TBI and non-severe TBD highlights the challenge of differentiating infection from early disease, strengthening the need for multi-biomarker approaches. Overall, subgroup analysis revealed that severe TB drives host protein changes, while non-severe TB shows intermediate profiles between infection and severe disease. This emphasizes both the clinical progress of TB and the value of severity-based stratification in biomarker discovery and clinical translation.

This study has several limitations that should be acknowledged. First, the reduced number of mice and human subjects may limit the statistical power and generalization of the findings, and larger cohorts will be needed to validate these results. Second, the interpretation of ferritin levels is limited by the lack of specificity of the commercial ELISA kits, which do not discriminate between the two types of subunits. Consequently, potential differences in the ratios of the subunits would not be captured by this assay. This limitation would also apply if such assays were to be used for diagnostic purposes, for example in the context of TB. Third, the proteomics panel employed was incomplete, restricting the number of iron-related proteins that could be assessed. Finally, principal component analysis (PCA) was performed on a reduced number of proteins, which may limit the robustness of the clustering and the extent to which the identified patterns reflect the full proteomic landscape [120]. Together, these factors highlight the need for more comprehensive and larger-scale studies to confirm and expand upon our observations.

This work directly supports the World Health Organization's vision of ending the global TB epidemic and aligns with the Sustainable Development Goal (SDG) 3.3, which aims to "*end the epidemics of AIDS, tuberculosis, malaria and neglected tropical*

diseases by 2030" [121]. Under the WHO's End TB Strategy, the global target is an 80% reduction in TB incidence and a 90% decrease in TB deaths by 2030 relative to 2015 numbers [122]. Our research contributes to this goal by adding some insights to diagnostic biomarker discovery, which is crucial for early identification and management of both infection and disease, especially among children and vulnerable populations. By enhancing diagnostic accuracy, particularly in resource-limited settings and in relation to iron-related comorbidities, our findings support more effective TB care, a goal in line with SDG Goal 3, focused on universal health coverage and quality healthcare access [121].

Conclusion

The purpose of this work was to investigate how *M. tuberculosis* infection alters host iron homeostasis and to evaluate the potential of circulating iron-associated proteins as biomarkers for tuberculosis (TB) diagnosis and disease progression. Given that mycobacteria are intramacrophagic pathogens that rely on host iron for survival, understanding host-pathogen competition for iron is essential for both mechanistic insight and translational applications.

Our findings demonstrate that infection and inflammation lead to distinct changes in circulating proteins, with ferritin heavy chain (FTH) having higher sensitivity to inflammatory stimuli, and ferritin light chain (FTL) responding primarily to elevated iron levels. This differential regulation suggests that measurement of ferritin subunits can help distinguish between TB-associated inflammation and iron overload disorders. Moreover, severe TB disease was characterized by increases in inflammatory cytokines, elevated TFR1 expression, and a tendency for ferritin, particularly L-ferritin, upregulation. These results revealed the potential of iron-related and immune proteins as diagnostic biomarkers for TB disease progression. While inflammatory proteins appear to be the most reliable diagnostic biomarkers, the addition of iron-related markers may offer valuable information for assessing disease progression and severity.

Nonetheless, the study has important limitations. The reduced number of mice and human subjects restricted statistical power, and the incomplete proteomics panel limited the scope of the host response captured. Additionally, PCA was conducted on a reduced protein set, which may have limited the robustness of the clustering. These limitations emphasize the need for larger, more extensive studies to validate our findings.

Future work should expand iron-related proteomic coverage and integrate ferritin subunit measurements with immune and metabolic markers. Such approaches will be essential to refine biomarker panels capable of distinguishing infection from early disease and stratifying patients according to severity. Ultimately, this line of research contributes to the World Health Organization’s End TB Strategy and the Sustainable Development Goal 3.3 by advancing biomarker-driven diagnostics that can support earlier detection, more precise diagnosis, and improved clinical management of TB, particularly in high-burden and resource-limited settings.

References

1. Rahlwes, K.C., et al., *Pathogenicity and virulence of Mycobacterium tuberculosis.* Virulence, 2023. **14**(1): p. 2150449.
2. Chai, Q., Y. Zhang, and C.H. Liu, *Mycobacterium tuberculosis: An Adaptable Pathogen Associated With Multiple Human Diseases.* Front Cell Infect Microbiol, 2018. **8**: p. 158.
3. Organization, G.W.H., *Global tuberculosis report 2024*. 2024.
4. Kanabalan, R.D., et al., *Human tuberculosis and Mycobacterium tuberculosis complex: A review on genetic diversity, pathogenesis and omics approaches in host biomarkers discovery.* Microbiological Research, 2021. **246**: p. 126674.
5. Gomes, A.C., et al., *IFN-γ-Dependent Reduction of Erythrocyte Life Span Leads to Anemia during Mycobacterial Infection.* J Immunol, 2019. **203**(9): p. 2485-2496.
6. Orgeur, M., et al., *Evolution and emergence of Mycobacterium tuberculosis.* FEMS Microbiology Reviews, 2024. **48**(2).
7. Glickman, M.S. and W.R. Jacobs, Jr., *Microbial pathogenesis of Mycobacterium tuberculosis: dawn of a discipline.* Cell, 2001. **104**(4): p. 477-85.
8. Podinovskaia, M., et al., *Infection of macrophages with Mycobacterium tuberculosis induces global modifications to phagosomal function.* Cell Microbiol, 2013. **15**(6): p. 843-59.
9. Bartolomeu-Gonçalves, G., et al., *Tuberculosis Diagnosis: Current, Ongoing, and Future Approaches.* Diseases, 2024. **12**(9).
10. Mukherjee, S., et al., *Evolution of tuberculosis diagnostics: From molecular strategies to nanodiagnostics.* Tuberculosis, 2023. **140**: p. 102340.
11. Shamaei, M. and M. Mirsaeidi, *Nontuberculous Mycobacteria, Macrophages, and Host Innate Immune Response.* Infect Immun, 2021. **89**(8): p. e0081220.
12. Abe, Y., et al., *Host Immune Response and Novel Diagnostic Approach to NTM Infections.* Int J Mol Sci, 2020. **21**(12).
13. Prasla, Z., R.L. Sutliff, and R.T. Sadikot, *Macrophage Signaling Pathways in Pulmonary Nontuberculous Mycobacteria Infections.* Am J Respir Cell Mol Biol, 2020. **63**(2): p. 144-151.
14. Ignatov, D., et al., *Mycobacterium avium-triggered diseases: pathogenomics.* Cell Microbiol, 2012. **14**(6): p. 808-18.
15. Verma, D., E.D. Chan, and D.J. Ordway, *The double-edged sword of Tregs in M tuberculosis, M avium, and M absessus infection.* Immunol Rev, 2021. **301**(1): p. 48-61.
16. Pantopoulos, K., et al., *Mechanisms of mammalian iron homeostasis.* Biochemistry, 2012. **51**(29): p. 5705-24.
17. Hollerer, I., A. Bachmann, and M.U. Muckenthaler, *Pathophysiological consequences and benefits of HFE mutations: 20 years of research.* Haematologica, 2017. **102**(5): p. 809-817.
18. Sousa Gerós, A., et al., *The battle for iron in enteric infections.* Immunology, 2020. **161**(3): p. 186-199.
19. Camaschella, C., A. Nai, and L. Silvestri, *Iron metabolism and iron disorders revisited in the hepcidin era.* Haematologica, 2020. **105**(2): p. 260-272.
20. Fonseca, Ó., et al., *New Perspectives on Circulating Ferritin: Its Role in Health and Disease.* Molecules, 2023. **28**(23).
21. Charlebois, E., et al., *A crosstalk between hepcidin and IRE/IRP pathways controls ferroportin expression and determines serum iron levels in mice.* Elife, 2022. **11**.
22. Pogoutse, A.K. and T.F. Moraes, *Iron acquisition through the bacterial transferrin receptor.* Crit Rev Biochem Mol Biol, 2017. **52**(3): p. 314-326.
23. Muckenthaler, M.U., et al., *A Red Carpet for Iron Metabolism.* Cell, 2017. **168**(3): p. 344-361.

24. Kawabata, H., *Transferrin and transferrin receptors update.* Free Radic Biol Med, 2019. **133**: p. 46-54.
25. Wang, C.Y. and J.L. Babitt, *Liver iron sensing and body iron homeostasis.* Blood, 2019. **133**(1): p. 18-29.
26. Dassler, K., et al., *Release of the Soluble Transferrin Receptor Is Directly Regulated by Binding of Its Ligand Ferritransferrin*.* Journal of Biological Chemistry, 2006. **281**(6): p. 3297-3304.
27. Gehrer, C.M., et al., *Advances in Ferritin Physiology and Possible Implications in Bacterial Infection.* Int J Mol Sci, 2023. **24**(5).
28. Beaumont, C., et al., *Transcriptional regulation of ferritin H and L subunits in adult erythroid and liver cells from the mouse. Unambiguous identification of mouse ferritin subunits and in vitro formation of the ferritin shells.* J Biol Chem, 1989. **264**(13): p. 7498-504.
29. Dickey, L.F., et al., *Differences in the regulation of messenger RNA for housekeeping and specialized-cell ferritin. A comparison of three distinct ferritin complementary DNAs, the corresponding subunits, and identification of the first processed in amphibia.* Journal of Biological Chemistry, 1987. **262**(16): p. 7901-7907.
30. Cohen, L.A., et al., *Serum ferritin is derived primarily from macrophages through a nonclassical secretory pathway.* Blood, 2010. **116**(9): p. 1574-1584.
31. Watanabe, K., et al., *Iron Content of Rat Serum Ferritin.* Journal of Veterinary Medical Science, 2001. **63**(5): p. 587-589.
32. Kell, D.B. and E. Pretorius, *Serum ferritin is an important inflammatory disease marker, as it is mainly a leakage product from damaged cells.* Metallomics, 2014. **6**(4): p. 748-773.
33. Moreira, A.C., G. Mesquita, and M.S. Gomes, *Ferritin: An Inflammatory Player Keeping Iron at the Core of Pathogen-Host Interactions.* Microorganisms, 2020. **8**(4).
34. Hsu, M.Y., et al., *Iron: An Essential Element of Cancer Metabolism.* Cells, 2020. **9**(12).
35. Nairz, M., et al., *Cell-specific expression of Hfe determines the outcome of Salmonella enterica serovar Typhimurium infection in mice.* Haematologica, 2021. **106**(12): p. 3149-3161.
36. Gomes, A.C., et al., *Modulation of Iron Metabolism in Response to Infection: Twists for All Tastes.* Pharmaceuticals (Basel), 2018. **11**(3).
37. Marques, O., G. Weiss, and M.U. Muckenthaler, *The role of iron in chronic inflammatory diseases: from mechanisms to treatment options in anemia of inflammation.* Blood, 2022. **140**(19): p. 2011-2023.
38. Ni, S., et al., *Iron Metabolism and Immune Regulation.* Front Immunol, 2022. **13**: p. 816282.
39. Zhang, L., et al., *Comprehensive analysis of iron utilization by Mycobacterium tuberculosis.* PLoS Pathog, 2020. **16**(2): p. e1008337.
40. Chao, A., et al., *Iron Acquisition in Mycobacterium tuberculosis.* Chem Rev, 2019. **119**(2): p. 1193-1220.
41. Baatjies, L., A.G. Loxton, and M.J. Williams, *Host and Bacterial Iron Homeostasis, an Underexplored Area in Tuberculosis Biomarker Research.* Front Immunol, 2021. **12**: p. 742059.
42. Wilson, B.R., et al., *Siderophores in Iron Metabolism: From Mechanism to Therapy Potential.* Trends Mol Med, 2016. **22**(12): p. 1077-1090.
43. Lambrecht, R.S. and M.T. Collins, *Inability to detect mycobactin in mycobacteria-infected tissues suggests an alternative iron acquisition mechanism by mycobacteria in vivo.* Microb Pathog, 1993. **14**(3): p. 229-38.
44. Tullius, M.V., et al., *A Replication-Limited Recombinant Mycobacterium bovis BCG vaccine against tuberculosis designed for human immunodeficiency virus-*

positive persons is safer and more efficacious than BCG. Infect Immun, 2008. **76**(11): p. 5200-14.
45. Schaible , U.E., et al., *Correction of the Iron Overload Defect in β-2-Microglobulin Knockout Mice by Lactoferrin Abolishes Their Increased Susceptibility to Tuberculosis.* Journal of Experimental Medicine, 2002. **196**(11): p. 1507-1513.
46. Lounis, N., et al., *Impact of iron loading and iron chelation on murine tuberculosis.* Clinical Microbiology and Infection, 1999. **5**(11): p. 687-692.
47. Boelaert, J.R., et al., *The Effect of the Host's Iron Status on Tuberculosis.* The Journal of Infectious Diseases, 2007. **195**(12): p. 1745-1753.
48. Tanner, R., et al., *The influence of haemoglobin and iron on in vitro mycobacterial growth inhibition assays.* Scientific Reports, 2017. **7**(1): p. 43478.
49. Moreira, A.C., et al., *H-Ferritin Produced by Myeloid Cells Is Released to the Circulation and Plays a Major Role in Liver Iron Distribution during Infection.* Int J Mol Sci, 2021. **23**(1).
50. Moreira Ana, C., et al., *Hepcidin-(In)dependent Mechanisms of Iron Metabolism Regulation during Infection by Listeria and Salmonella.* Infection and Immunity, 2017. **85**(9): p. 10.1128/iai.00353-17.
51. Moreira, A.C., et al., *Iron Related Biomarkers Predict Disease Severity in a Cohort of Portuguese Adult Patients during COVID-19 Acute Infection.* Viruses, 2021. **13**(12): p. 2482.
52. Dai, Y., et al., *Biomarkers of iron metabolism facilitate clinical diagnosis in Mycobacterium tuberculosis infection.* Thorax, 2019. **74**(12): p. 1161-1167.
53. Lim, D., et al., *The hepcidin-ferroportin axis controls the iron content of Salmonella-containing vacuoles in macrophages.* Nat Commun, 2018. **9**(1): p. 2091.
54. Sow, F.B., et al., *Hepcidin is synergistically induced in mouse macrophages by mycobacteria and IFN-γ, and is present in the mycobacterial phagosome (B166).* The Journal of Immunology, 2007. **178**(1_Supplement): p. LB35-LB35.
55. Rodrigues, P.N., et al., *Mycobacteria-induced anaemia revisited: A molecular approach reveals the involvement of NRAMP1 and lipocalin-2, but not of hepcidin.* Immunobiology, 2011. **216**(10): p. 1127-1134.
56. Harrington-Kandt, R., et al., *Hepcidin deficiency and iron deficiency do not alter tuberculosis susceptibility in a murine M.tb infection model.* PLoS One, 2018. **13**(1): p. e0191038.
57. Silva-Gomes, S., et al., *Mycobacterium avium infection induces H-ferritin expression in mouse primary macrophages by activating Toll-like receptor 2.* PLoS One, 2013. **8**(12): p. e82874.
58. Reddy, V.P., et al., *Ferritin H Deficiency in Myeloid Compartments Dysregulates Host Energy Metabolism and Increases Susceptibility to Mycobacterium tuberculosis Infection.* Front Immunol, 2018. **9**: p. 860.
59. Ullah, I. and M. Lang, *Key players in the regulation of iron homeostasis at the host-pathogen interface.* Front Immunol, 2023. **14**: p. 1279826.
60. Nogueira, B.M.F., et al., *Diagnostic biomarkers for active tuberculosis: progress and challenges.* EMBO Mol Med, 2022. **14**(12): p. e14088.
61. Group, F.-N.B.W., in *BEST (Biomarkers, EndpointS, and other Tools) Resource*. 2016, Food and Drug Administration (US)
National Institutes of Health (US): Silver Spring (MD)
Bethesda (MD).
62. Califf, R.M., *Biomarker definitions and their applications.* Exp Biol Med (Maywood), 2018. **243**(3): p. 213-221.
63. Mousavian, Z., G. Källenius, and C. Sundling, *From simple to complex: Protein-based biomarker discovery in tuberculosis.* Eur J Immunol, 2023. **53**(12): p. e2350485.

64. Cui, M., C. Cheng, and L. Zhang, *High-throughput proteomics: a methodological mini-review.* Lab Invest, 2022. **102**(11): p. 1170-1181.
65. Organization, G.W.H., *WHO consolidated guidelines on tuberculosis.* 2024.
66. Correia-Neves, M., et al., *Lipoarabinomannan in Active and Passive Protection Against Tuberculosis.* Front Immunol, 2019. **10**: p. 1968.
67. Santambrogio, P., et al., *Functional and Immunological Analysis of Recombinant Mouse H- and L-Ferritins from Escherichia coli.* Protein Expression and Purification, 2000. **19**(1): p. 212-218.
68. Wik, L., et al., *Proximity Extension Assay in Combination with Next-Generation Sequencing for High-throughput Proteome-wide Analysis.* Mol Cell Proteomics, 2021. **20**: p. 100168.
69. Mesquita, G., et al., *H-Ferritin is essential for macrophages' capacity to store or detoxify exogenously added iron.* Scientific Reports, 2020. **10**(1): p. 3061.
70. Prieto, J., M. Barry, and S. Sherlock, *Serum ferritin in patients with iron overload and with acute and chronic liver diseases.* Gastroenterology, 1975. **68**(3): p. 525-33.
71. Adams, P.C. and J.C. Barton, *A diagnostic approach to hyperferritinemia with a non-elevated transferrin saturation.* Journal of Hepatology, 2011. **55**(2): p. 453-458.
72. Kernan, K.F. and J.A. Carcillo, *Hyperferritinemia and inflammation.* Int Immunol, 2017. **29**(9): p. 401-409.
73. Torti, F.M. and S.V. Torti, *Regulation of ferritin genes and protein.* Blood, 2002. **99**(10): p. 3505-16.
74. Boradia, V.M., et al., *Mycobacterium tuberculosis acquires iron by cell-surface sequestration and internalization of human holo-transferrin.* Nature Communications, 2014. **5**(1): p. 4730.
75. Gulhar, R., M.A. Ashraf, and I. Jialal, *Physiology, Acute Phase Reactants*, in *StatPearls*. 2025, StatPearls Publishing
Copyright © 2025, StatPearls Publishing LLC.: Treasure Island (FL).
76. Huntoon, K.M., et al., *The acute phase protein haptoglobin regulates host immunity.* J Leukoc Biol, 2008. **84**(1): p. 170-81.
77. Tsay, J., et al., *Bone loss caused by iron overload in a murine model: importance of oxidative stress.* Blood, 2010. **116**(14): p. 2582-9.
78. Gschwandtner, M., R. Derler, and K.S. Midwood, *More Than Just Attractive: How CCL2 Influences Myeloid Cell Behavior Beyond Chemotaxis.* Front Immunol, 2019. **10**: p. 2759.
79. Liu, M., et al., *CXCL10/IP-10 in infectious diseases pathogenesis and potential therapeutic implications.* Cytokine Growth Factor Rev, 2011. **22**(3): p. 121-30.
80. Schroder, K., et al., *Interferon-gamma: an overview of signals, mechanisms and functions.* J Leukoc Biol, 2004. **75**(2): p. 163-89.
81. Dinarello, C.A., *Interleukin-1 in the pathogenesis and treatment of inflammatory diseases.* Blood, 2011. **117**(14): p. 3720-32.
82. Tanaka, T., M. Narazaki, and T. Kishimoto, *IL-6 in inflammation, immunity, and disease.* Cold Spring Harb Perspect Biol, 2014. **6**(10): p. a016295.
83. Moore, K.W., et al., *Interleukin-10 and the Interleukin-10 Receptor.* Annual Review of Immunology, 2001. **19**(Volume 19, 2001): p. 683-765.
84. Trinchieri, G., *Interleukin-12 and the regulation of innate resistance and adaptive immunity.* Nature Reviews Immunology, 2003. **3**(2): p. 133-146.
85. Ihim, S.A., et al., *Interleukin-18 cytokine in immunity, inflammation, and autoimmunity: Biological role in induction, regulation, and treatment.* Front Immunol, 2022. **13**: p. 919973.
86. Vinay, D.S. and B.S. Kwon, *The tumour necrosis factor/TNF receptor superfamily: therapeutic targets in autoimmune diseases.* Clin Exp Immunol, 2011. **164**(2): p. 145-57.

87. Platanias, L.C., *Mechanisms of type-I- and type-II-interferon-mediated signalling.* Nature Reviews Immunology, 2005. **5**(5): p. 375-386.
88. Andriopoulos, B., Jr., et al., *BMP6 is a key endogenous regulator of hepcidin expression and iron metabolism.* Nat Genet, 2009. **41**(4): p. 482-7.
89. Babitt, J.L., et al., *Bone morphogenetic protein signaling by hemojuvelin regulates hepcidin expression.* Nat Genet, 2006. **38**(5): p. 531-9.
90. Ryter, S.W. and A.M. Choi, *Heme oxygenase-1/carbon monoxide: from metabolism to molecular therapy.* Am J Respir Cell Mol Biol, 2009. **41**(3): p. 251-60.
91. Wallace, D.F., *The Regulation of Iron Absorption and Homeostasis.* Clin Biochem Rev, 2016. **37**(2): p. 51-62.
92. Wakabayashi, H., et al., *Inhibitory effects of lactoferrin on growth and biofilm formation of Porphyromonas gingivalis and Prevotella intermedia.* Antimicrob Agents Chemother, 2009. **53**(8): p. 3308-16.
93. Donovan, A., et al., *The iron exporter ferroportin/Slc40a1 is essential for iron homeostasis.* Cell Metab, 2005. **1**(3): p. 191-200.
94. Zhang, X., et al., *Bach1: Function, Regulation, and Involvement in Disease.* Oxid Med Cell Longev, 2018. **2018**: p. 1347969.
95. Greenacre, M., et al., *Principal component analysis.* Nature Reviews Methods Primers, 2022. **2**(1): p. 100.
96. Jolliffe, I.T. and J. Cadima, *Principal component analysis: a review and recent developments.* Philos Trans A Math Phys Eng Sci, 2016. **374**(2065): p. 20150202.
97. Mousavian, Z., et al., *A protein signature associated with active tuberculosis identified by plasma profiling and network-based analysis.* iScience, 2022. **25**(12): p. 105652.
98. Cassat, J.E. and E.P. Skaar, *Iron in infection and immunity.* Cell Host Microbe, 2013. **13**(5): p. 509-519.
99. Kumar, N.P., et al., *Modulation of iron status biomarkers in tuberculosis-diabetes co-morbidity.* Tuberculosis, 2018. **108**: p. 127-135.
100. Wong, K. and P.C. Adams, *The diversity of liver diseases among outpatient referrals for an elevated serum ferritin.* Can J Gastroenterol, 2006. **20**(7): p. 467-70.
101. Sheldon, J.R., H.A. Laakso, and D.E. Heinrichs, *Iron Acquisition Strategies of Bacterial Pathogens.* Microbiol Spectr, 2016. **4**(2).
102. Ru, Q., et al., *Iron homeostasis and ferroptosis in human diseases: mechanisms and therapeutic prospects.* Signal Transduction and Targeted Therapy, 2024. **9**(1): p. 271.
103. Chai, Q., Z. Lu, and C.H. Liu, *Host defense mechanisms against Mycobacterium tuberculosis.* Cell Mol Life Sci, 2020. **77**(10): p. 1859-1878.
104. Reddy, V.P., et al. *Ferritin H Deficiency in Myeloid Compartments Dysregulates Host Energy Metabolism and Increases Susceptibility to <i>Mycobacterium tuberculosis</i> Infection*. Frontiers in immunology, 2018. **9**, 860 DOI: 10.3389/fimmu.2018.00860.
105. LEGGETT, B.A., et al., *Differential regulation of ferritin H and L subunit mRNA during inflammation and long-term iron overload.* Journal of Gastroenterology and Hepatology, 1993. **8**(1): p. 21-27.
106. Sammarco, M.C., et al., *Ferritin L and H subunits are differentially regulated on a post-transcriptional level.* J Biol Chem, 2008. **283**(8): p. 4578-87.
107. Minchella, P.A., et al., *Iron homeostasis and progression to pulmonary tuberculosis disease among household contacts.* Tuberculosis (Edinb), 2015. **95**(3): p. 288-93.
108. Sproston, N.R. and J.J. Ashworth, *Role of C-Reactive Protein at Sites of Inflammation and Infection.* Front Immunol, 2018. **9**: p. 754.

109. Leboueny, M., et al., *Changes of C-reactive protein and Procalcitonin after four weeks of treatment in patients with pulmonary TB.* J Clin Tuberc Other Mycobact Dis, 2023. **31**: p. 100348.
110. Tishkowski, K. and M. Zubair, *Erythrocyte Sedimentation Rate*, in *StatPearls*. 2025, StatPearls Publishing
Copyright © 2025, StatPearls Publishing LLC.: Treasure Island (FL).
111. Markanday, A., *Acute Phase Reactants in Infections: Evidence-Based Review and a Guide for Clinicians.* Open Forum Infect Dis, 2015. **2**(3): p. ofv098.
112. Flynn, J.L., J. Chan, and P.L. Lin, *Macrophages and control of granulomatous inflammation in tuberculosis.* Mucosal Immunology, 2011. **4**(3): p. 271-278.
113. Matsuyama, M., et al., *The Role of NRF2 in Mycobacterial Infection.* Antioxidants, 2021. **10**(12): p. 1861.
114. Kaushik, S.R., et al., *Low circulatory Fe and Se levels with a higher IL-6/IL-10 ratio provide nutritional immunity in tuberculosis.* Frontiers in Immunology, 2023. **Volume 13 - 2022**.
115. Guo, Q., et al., *Transferrin receptors.* Experimental & Molecular Medicine, 2025. **57**(4): p. 724-732.
116. Li, L., et al., *Binding and uptake of H-ferritin are mediated by human transferrin receptor-1.* Proc Natl Acad Sci U S A, 2010. **107**(8): p. 3505-10.
117. Minchella, P.A., et al., *Complex anemia in tuberculosis: the need to consider causes and timing when designing interventions.* Clin Infect Dis, 2015. **60**(5): p. 764-72.
118. Dai, Y., et al., *Mycobacterium tuberculosis induces host autophagic ferritin degradation for enhanced iron bioavailability and bacterial growth.* Autophagy, 2024. **20**(4): p. 943-945.
119. Miranda, P., et al., *Sustained elevated levels of C-reactive protein and ferritin in pulmonary tuberculosis patients remaining culture positive upon treatment initiation.* PLoS One, 2017. **12**(4): p. e0175278.
120. Yao, Y. and A. Ochoa, *Limitations of principal components in quantitative genetic association models for human studies.* Elife, 2023. **12**.
121. Assembly, S.s.U.N.G., *Transforming our world: the 2030 Agenda for Sustainable Development*. 2015.
122. (WHO), W.H.O. *SDG Target 3.3 Communicable diseases* [cited 2025 22nd August]; Available from: https://www.who.int/data/gho/data/themes/topics/sdg-target-3_3-communicable-diseases.